European Polymer Journal 134 (2020) 109842

Contents lists available at ScienceDirect

European Polymer Journal

journal homepage: www.elsevier.com/locate/europolj

Tuning the conformation and mechanical properties of silk fibroin hydrogels

Narges Johari[a], Lorenzo Moroni[b,*], Ali Samadikuchaksaraei[c,d,e]

[a] Department of Materials Science and Engineering, Golpayegan University of Technology, Isfahan, Iran
[b] Maastricht University, MERLN Institute for Technology Inspired Regenerative Medicine, Complex Tissue Regeneration Department, Maastricht, the Netherlands
[c] Cellular and Molecular Research Center, Iran University of Medical Sciences, Tehran, Iran
[d] Department of Tissue Engineering & Regenerative Medicine, Faculty of Advanced Technologies in Medicine, Iran University of Medical Sciences, Tehran, Iran
[e] Department of Medical Biotechnology, Faculty of Allied Medicine, Iran University of Medical Sciences, Tehran, Iran

ARTICLE INFO

Keywords:
Silk fibroin
Treatment
Mechanical properties
β-sheet formation

ABSTRACT

Mechanical properties of biomaterials play an important role in their biological performance. Among the most important parameters in designing of biomaterials, their structure and conformation strongly affect their mechanical properties as well as cell adhesion, proliferation, and differentiation. Silk fibroin (SF), extracted from *Bombyx mori* cocoons, has attracted a lot of scientific interest in the past years as a natural biomaterial due to its exceptional host tissues response, appropriate mechanical properties, tunable degradation, simple processing method and low cost. The formation of β-sheets in the structure of SF enhances its mechanical properties. In recent years, several studies have focused on tuning the mechanical properties of SF for biomedical applications by inducing the formation of β-sheets. Some treatment methods have been introduced to alter SF structure and improve its mechanical properties. Chemical, physical and enzymatic crosslinking, water and alcoholic treatments and irradiations have been recommended as methods to inducing β-sheets conformation in SF structure. Several studies have developed these methods by adding suitable components and changing the concentration, temperature, humidity, pH, and various other parameters. In this review, we focus on the treatment methods, which result in the conformational transition of SF and tuning its mechanical properties.

1. Introduction

The critical roles of cell-matrix interactions in cell biological processes, such as adhesion, growth, differentiation and apoptosis has been the focus of several investigations [1,2]. Mechanical properties of biomaterials and tissue extracellular matrix (ECM) are among the most important factors in tissue engineering. Namely, the elastic modulus, or stiffness of biomaterials and tissue ECM vary in a broad range between 3 kPa and several GPa [3,4]. Further, the stiffness is known to significantly impact the differentiation of stem cells and maintenance of cell functionality in soft tissue engineering [5]. Researches confirmed that ECM's mechanical properties can actively influence the differentiation of stem cells into various cell types, such as neurons, myoblasts and osteoblasts [6]. Therefore, many biomaterials, in particular hydrogels, can be developed with the capacity to adjust their stiffness [6–8]. Considering the wide range of stiffness in diverse tissues, various protocols, such as blending and crosslinking different polymers and components, were developed to modulate the stiffness of various tissues [9,10].

In recent years, due to high water content, non-toxicity, excellent biological performance, and intrinsic biocompatibility, hydrogels have been widely used in various biomedical applications including drug delivery, contact lenses, cell encapsulation materials, wound dressings, and tissue engineering scaffolds [11–16]. Based on the source, hydrogels are classified into synthetic and natural [17]. Synthetic hydrogels are hydrophobic with strong chemical bonds, resulting in slow degradation rate and high mechanical strength, while cells cannot often attach to them [17–19]. Yet, natural hydrogels have been utilized in various biomedical applications because of their inherent biodegradability, critical biological performances, natural extracellular matrix components and biocompatibility. However, their potential immunogenic reactions and poor mechanical properties have restricted natural hydrogels applications [16,18,20–22]. Indeed, the main drawback of hydrogels is the inherent weakness, which mainly limits their applications to soft and hard tissues. Therefore, several studies have been performed to modify hydrogels to obtain excellent mechanical properties [23–25]. Various methods have been applied to improve the mechanical properties of polymer-based hydrogels, such as those containing agarose, gelatin, hyaluronic acid, pluronic and silk fibroin [26–28]. Chemical crosslinking was used as a well-known strategy to

* Corresponding author.
E-mail address: l.moroni@maastrichtuniversity.nl (L. Moroni).

https://doi.org/10.1016/j.eurpolymj.2020.109842
Received 11 February 2020; Received in revised form 3 June 2020; Accepted 9 June 2020
Available online 12 June 2020

increase the mechanical properties of hydrogels, although the cytocompatibility of chemical crosslinking agents remains a challenging issue [29]. In addition to chemical crosslinking, physical treatments [30] and blending with other natural or synthetic polymers [26,31] have been employed to improve the mechanical properties of hydrogels, contributing to their improved safety.

Silk fibroin (SF) is a natural polymer with various appealing properties, such as appropriate host response, minimal inflammatory reactions and tunable biodegradability, which is applied as a cell-support matrix for stem cells, fibroblasts, nerve cells, and osteoblasts, and as a scaffold for different tissues, including bone, cartilage, skin, nerve and blood vessel, due to its similarity to the ECM [32–38]. The native ECM is composed of a nanofibrous structure made of proteins and polysaccharides. Therefore, using proteins and polysaccharides as biomaterials can mimic the ECM structure as well as improve cell attachment, proliferation and differentiation for tissue regeneration [39,40]. Accordingly, fibrous SF extracted from *Bombyx mori* cocoons is composed of heavy and light chains linked by a disulfide bond. The primary high molar-mass structure of SF consists of the amino acid sequence as Gly-Ser-Gly-Ala-Gly-Ala, which can crystallize as the stable anti-parallel β-sheets and improve the rigidity and the tensile strength of SF. On the other hand, 70% of the β-sheet crystalline structure of SF is composed of the protein structure surrounded by hydrophilic and non-repetitive amorphous regions [41,42]. SF can be prepared via a water-based solution at room temperature with a neutral pH and formed as α-helix and random coils, exhibiting relatively poor mechanical properties [43]. To improve the strength of SF, various treatment methods have been evaluated in recent years. Specifically, the formation of β-sheet structure has been introduced by enzymatic, chemical and physical crosslinking of SF hydrogels [44,45], because the process of hydrogelation results from the structural transitions from random coil to β-sheet [46–50]. Enzymatic crosslinkers, such as genipin, chemical crosslinkers, including, for instance glutaraldehyde and carbodiimide hydrochloride, and physical crosslinking methods, such as heating, vortex shearing, ultra-sonication or electric current, accelerate the hydrogelation of SF by providing the sufficient energy to overcome the energy barrier of β-sheet formation. Further, studies reported several processes developed to modify the stiffness of SF and improve its biological properties [45,49,51–56]. Indeed, additional biomaterials and β-sheet domains within SF matrix can improve its mechanical properties [57]. Briefly, the advantages and disadvantages of enzymatic, chemical and physical crosslinking method have been mentioned in Table 1.

The evaluation of treatment methods for transforming the structure of SF has opened new avenues for engineering silk materials for biomedical applications and improved mechanical properties for implanting these biomaterials into the damaged tissue. In recent decades, various treatment methods, such as chemical, physical and enzymatic crosslinking, irradiations and alcoholic treatment have been investigated to alter the random coil structure of SF into β-sheet conformation, resulting in an increase of mechanical properties for clinical applications. The purpose of this review is to summarize the recent advancements in modifying treatment methods, affecting the SF structure and mechanical properties.

2. Silk fibroin

Silk fibroin (SF) is a protein, derived from Bombyx mori cocoons and has been widely evaluated due to its outstanding biological response, tunable biodegradability and appropriate mechanical properties [59–61]. SF is an FDA-approved polymer for biomedical applications such as sutures, tissue regeneration, and drug delivery systems [62,63] The main conformations of SF are silk I and silk II, as well as the unstable silk III, which exists in SF solution at the air/water interface. Silk I is a metastable structure with a zigzag amorphous conformation, belonging to an orthorhombic system. Due to the presence of a dominant number of random coils and α-helix, silk I has the lowest crystallinity, resulting in its instability and water-solubility [42,64]. Silk II (β-sheets / β-turns) as an anti-parallel β-sheet conformation belongs to a monoclinic system and has the highest crystallinity, leading to its stability, water-insolubility, and thermal and mechanical resistance [42,63,65]. β-turns is an intermediate structure of SF which could be formed by tightening or close packing of loose structures [66]. Although, SF samples soaked in methanol show no such intermediate structure, because in the presence of methanol, dehydration of polypeptide chains induces β-sheet crystalline structure [66,67]. Silk III is a unique crystalline polymorph structure with a threefold helical crystal. Namely, it has a metastable structure with the crystallinity between Silk I and Silk II [63]. SF molecules possess the hydrophilic (Tyr, Ser) and hydrophobic (Gly, Ala) chain segments arranged alternately [42]. Hydrogen bonds between adjacent segments result in the rigidity and tensile strength of SF. Also, the structure of silk I can be easily converted to silk II via treatments and external stimuli, such as soaking in methanol and UV irradiation. [42,59,68,69]. In silk III, the free hydroxyl groups of Ser residues lead to line it up in the water, while Ala residues protrude to the air phase, making Ser hydrophilic and Ala hydrophobic columns parallel to the helical axis of SF [63]. Fig. 1 exhibits a schematic representation of the SF molecular chain showing the hydrogen bonding and structures [59]. The conformational transitions and crystallinity content of SF extremely affect its physio-chemical and mechanical properties, impacting on its biological properties and applications [59,65]. The secondary structure of SF (silk II) plays an important role on its physico-chemical properties and provide its mechanical stabilities, while silk I has more appropriate host responses than silk II [65,70].

3. Enzyme-catalyzed crosslinking of SF

Prior researches illustrated that by changing the molecular weight and the solvent composition, the stiffness of SF can be controlled in the range of 200–10,000 Pa [71,72]. Hence, Taddei *et al.* [54] crosslinked silk fibroin/gelatin (SF/G) films by microbial transglutaminase (mTG) and mushroom tyrosinase (MT). The mechanical properties in the

Table 1
Advantages and dis advantages of the physical, enzymatic and chemical crosslinking methods [58].

Crosslinking method	Advantages	Disadvantages
Physical	Safe less toxic for cells than chemical agents inexpensive minimum tissue reaction after crosslinking process	Bonds are weaker than with chemical crosslinkers may alter the properties of the materials needs more time for crosslinking lack of control over the reaction kinetics of crosslinking
Enzymatic	Unlike many chemical crosslinkers, enzymes are most active under mild aqueous reaction conditions crosslinking process can often be controlled by modifying temperatures, pH, or ionic strength	The most expensive crosslinker substrate specificity
Chemical	Forming very strong bonds	Cell toxicity remains to be tested needs washing to remove the residual crosslinker more expensive than physical crosslinker

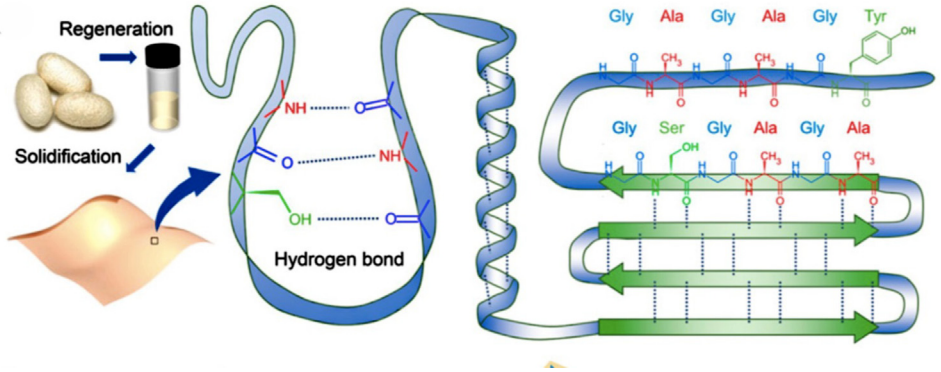

Fig. 1. Schematic representation of SF molecular chain showing the hydrogen bonding and SF structures (random coil, helix and β-sheet, respectively). Reused with permission [59]. Copyright 2019, PNAS.

tensile assay displayed elongation at break, elastic modulus and ultimate tensile strength of pure SF measured as 1.3%, 3.1 GPa and 22.8 MPa in average respectively, while for uncrosslinked SF/G films these properties were determined as 3.2%, 4.6 GPa and 89.4 MPa, in average respectively. However, the mechanical performance of enzymatically crosslinked SF and SF/G films with mTG and MT decreased compared to uncrosslinked samples. For instance, the elongation at break, elastic modulus and ultimate tensile strength of the enzyme crosslinked SF/G films were measured in the range of 2.7–3.2%, 3.5–4.9 GPa and 68.8–96.5 MPa, respectively. Furthermore, in several studies, horseradish peroxidase (HRP) and hydrogen peroxide (H_2O_2) were used as an enzyme catalyzed crosslinker of SF to form hydrogels, providing high elasticity and tunable stiffness [73–75]. Partlow *et al.* [73] revealed a new method for covalently crosslinking tyrosine residues in silk fibroin via HRP and H_2O_2. These polymers exhibit high elasticity, shear strains around 100%, compressive strains greater than 70% and stiffness between 200 and 10,000 Pa, which are appropriate for soft tissues. Indeed, HRP crosslinking of SF in the presence of H_2O_2 leads to the formation of a stable, highly elastic, and transparent gel, since HRP facilitates crosslinking of the tyrosines in SF via the formation of free radicals in the presence of H_2O_2 [76]. The main products of the general reaction are two water molecules and two phenolic radicals. Then, tyrosine radicals form during the HRP catalyzed reaction and react with each other to form covalent bonds [77]. Notably, dityrosine bonds have been found in Tussah silk fibroin, however were not shown in the *Bombyx mori* fibroin [78], investigated by Partlow *et al.* [73]. Therefore, this research revealed that the covalent dityrosine bonds of SF hydrogels prepared a strong hydrogel network with high stiffness and excellent elasticity. Fig. 2 exhibits a proposed reaction pathway for HRP/H_2O_2 crosslinking of SF [75]. Furthermore, the control over HRP and H_2O_2 may result in further fine tuning of SF hydrogels [73].

Yan *et al.* [79] synthesized a core–shell structure of SF by soaking the enzymatically crosslinked SF hydrogels via peroxidase-mediated into methanol. By increasing the soaking time from 1 to 10 min, the shell thickness increased from around 200 μm to around 850 μm, resulted in improving the compressive modulus of SF core–shell hydrogels from around 22 kPa to around 1.12 MPa. Indeed, due to the soaking of core–shell hydrogels in methanol as a fast conformational transition inducer, the conformation of the shell and core layers was different and became dominant β-sheet and random coil, respectively [79–81].

Next, Ribeiro *et al.* [82] developed stimuli-responsive HRP crosslinked SF hydrogels reacted at physiological conditions. The rheological properties of SF hydrogels and SF/HRP/H_2O_2 mixture before and after gelation revealed that the storage modulus (G′) was higher than the loss modulus (G″); namely the prepared hydrogels showed to be viscoelastic, both in their amorphous and β-sheet conformations. The high concentrated SF solution (16 wt%) and enzyme (HRP) content lead to short gelation time, high water content and swelling ability, both in the amorphous and β-sheet states, protecting the hydrogel integrity and improving its ability to more closely simulate the physiological environment [79]. Indeed, the increase of contents of HRP and H_2O_2 enhances the amount of oxidized tyrosine groups and crosslinking degree, leading to improved mechanical properties of prepared hydrogels [83]. In addition, the investigation of rheological parameters exhibited that 3 days after hydrogelation in the presence of HRP/H_2O_2, showed random coil as the main structure of SF. From 3 days to 7 days after hydrogelation, β-sheet structural transitions occurred in SF, and after 10 days, β-sheet was the main conformation of SF hydrogels [82].

Wang *et al.* [84] developed bioactive SF hydrogels with tunable mechanical properties by crosslinking SF nanofibers via HRP according to the process reported by Partlow *et al.* [73]. Here, SF hydrogels were prepared by introducing inert silk fibroin nanofibers (SNF) through the enzyme crosslinked system of regenerated silk fibroin (RSF). Results revealed that the stiffness of prepared SNF-RSF hydrogels was considerably improved by changing the amount of SF nanofibers. SNF-RSF hydrogels illustrated various moduli in the range of 9.2–55 kPa, while the modulus of pure RSF hydrogels at the same concentration was around 1 KPa [84].

Recently, Ribeiro *et al.* [45] introduced bio-functional hierarchical scaffolds developed as an HRP-crosslinked SF (HRP-SF) and fully integrated into a ZnSr-doped β-tricalcium phosphate (HRP-SF/dTCP) layer for osteochondral tissue engineering. The results revealed that the ion-doped bi-layered scaffolds presented a wet compressive modulus of 226.56 ± 60.34 kPa and their dynamic mechanical properties were in the range from 403.56 ± 111.62 to 593.56 ± 206.90 kPa, while the wet compressive modulus and dynamic mechanical properties of the control bi-layered scaffolds were 189.18 ± 90.80 kPa and ranging from 262.72 ± 59.92 to 347.68 ± 93.37 kPa, respectively. Therefore, the results partly mimic the mechanical properties, existing at the cartilaginous side of the osteochondral tissue [85]. In another study, Chirila *et al.* [86] determined the gelation time of HRP/H_2O_2/SF using a rheological method, by measuring the dynamic moduli in oscillatory shear stress tests. The previous study confirmed that HRP-crosslinking of SF in aqueous condition results in the formation of chemical gels [75]. Here, the results demonstrated that for a specified amount of HRP and H_2O_2 in the reaction mixture, the gelation time was considerably reduced by increasing the concentration of SF [86].

4. Chemical and physical crosslinking of SF

Chemical crosslinking can enhance biopolymers functionality. Nowadays, low toxicity crosslinking agents, such as phenolic compounds and genipin have been used as food packaging materials [87].

For chemical crosslinking of SF, genipin and glutaraldehyde are commonly used as the crosslinking agents [88]. Silva *et al.* [71]

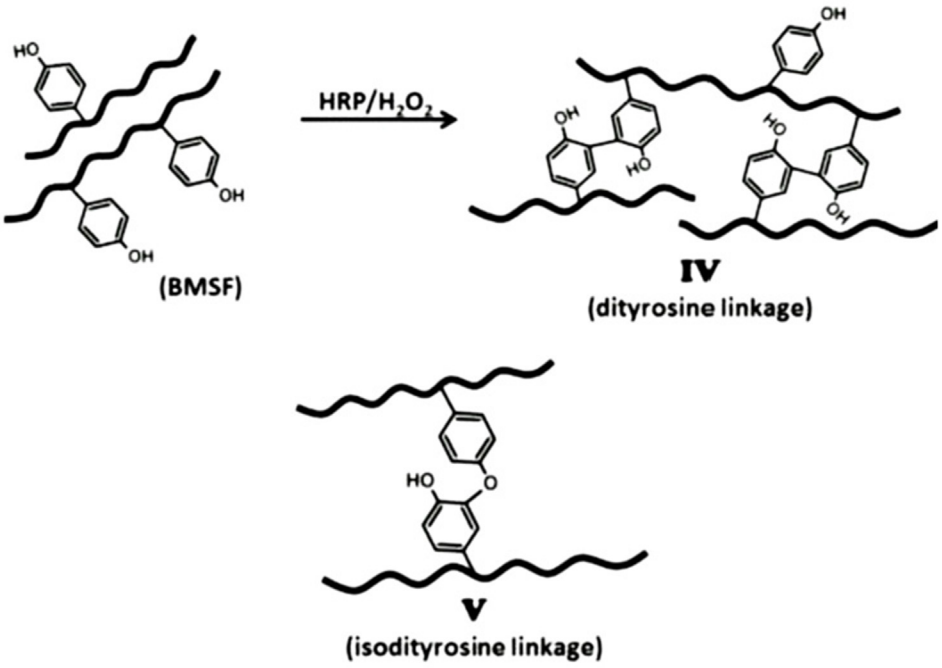

Fig. 2. The proposed reaction pathway for HRP/H_2O_2 crosslinking of SF. Reused with permission [75]. Copyright 2017, Wiley.

reported that genipin crosslinking promotes the formation of β-sheets in chitosan/silk fibroin/genipin sponges. Indeed, genipin crosslinking can increase the amount of sheets and leads to an increase in the amounts of crystalline domains. As a result, genipin crosslinking improves the stiffness and moduli of the matrix containing SF. Wang *et al.* [89] crosslinked SF films with glutaraldehyde to induce the conformational transition of SF from random coil to β-sheet and affect the interaction between the peptide chains of SF. The results showed that before crosslinking with glutaraldehyde, the tensile strength and elongation at break of the pure SF film were measured as 15.6 Mpa and 4.53%, in average respectively. However, by increasing the amount of glutaraldehyde, the tensile strength and elongation at break of the SF films were initially increased and then decreased, as the maximum values were exhibited in crosslinked SF films with about 7.5% glutaraldehyde and were 1.4 and 2.2 times of the pure SF ones, respectively. Indeed, the strength and flexibility of crosslinked SF films increase by increasing β-sheets content [89], while previous researchers illustrated that in contrast to the tensile strength, the flexibility of the crosslinked structures typically decreases by increasing the amount of β-sheets [90]. The results here, however, show that in the presence of glutaraldehyde, a reaction occurs in the amorphous regions of SF, containing amino acids, such as Lys, Arg, His, Asn and Gln [91], while the amount of amino acids is less than the added glutaraldehyde content. Therefore, several glutaraldehyde molecules remain unreacted or partially reacted in amorphous regions of SF, behaving as plasticizer to compensate for the negative effect of the increase in β-sheet structure on the flexibility of the prepared films [89]. Fig. 3 shows a schematic illustration of the effect of the plasticizers in polymer chains [87].

To improve the efficacy of glutaraldehyde crosslinked SF, Mohammadzadehmoghadam *et al.* [55] prepared SF/gelatin nanofiber mats with different blend ratios and crosslinked with glutaraldehyde vapor at room temperature, inducing the conformational transition of SF from random coils to β-sheets. SF/gelatin mats alone are limited due to their poor mechanical properties and unstable structures under physiological conditions [54,92]; crosslinking was applied using glutaraldehyde as the most common crosslinker with high efficiency in stabilizing collagenous materials [93]. Here, the results illustrated that the crosslinking degree was enhanced by increasing the gelatin content,

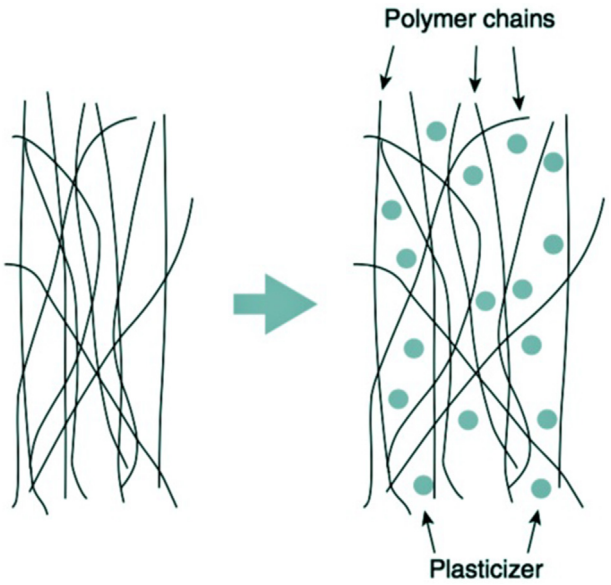

Fig. 3. The schematic illustration of the effect of the plasticizers in polymer chains. Reused with permission [87]. Copyright 2014, Elsevier.

altering from 34% for pure SF nanofiber mat to 43% for SF/gelatin one at the blend ratio of 70/30. The crosslinking degree directly affected mechanical properties of the nanofiber mats. By increasing the amount of gelatin from 10 to 30 wt% into SF, the tensile strength of SF/gelatin nanofiber mats was improved from 10 to 27% and Young's modulus increased from 12 to 27%, respectively [55]. Since by increasing the crosslinking degree with gelatin content the crosslinking density of prepared mats increases and molecular chains of proteins graft, the structural integration of SF/gelatin nanofibers results in increasing their mechanical properties [94–96]. However, the elongation at break of the prepared mats decreased from 20% for pure SF to 16% for SF/gelatin nanofiber mats blended in the ratio of 70/30 [55], due to increasing of the crosslinking density with gelatin content, which results in the fiber fusion and reduction of the porosity [97,98].

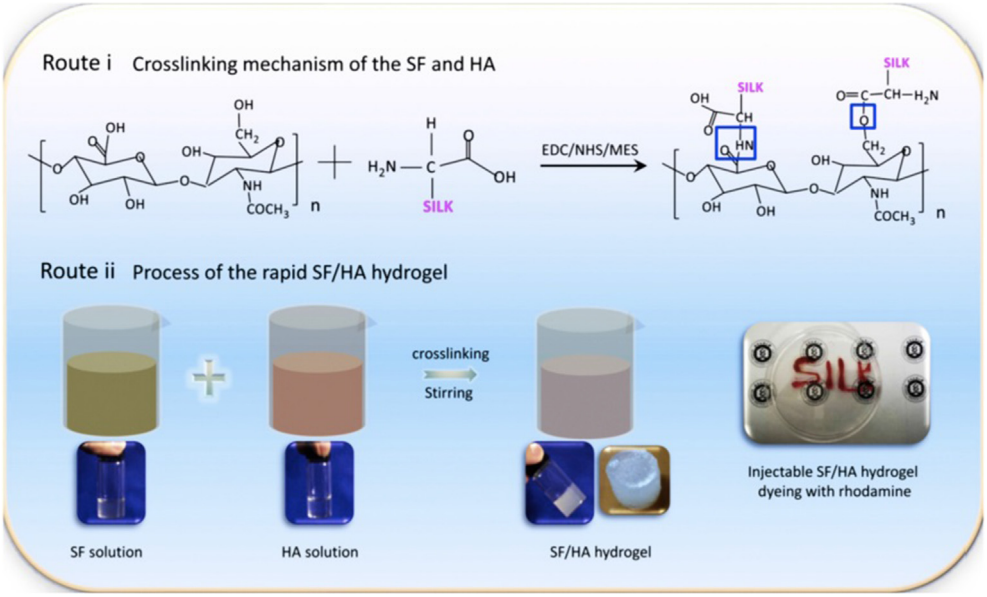

Fig. 4. The process of the formation of SF/HA hydrogel. Reused with permission [56]. Copyright 2018, Elsevier.

The most important disadvantage of chemical crosslinkers is their potential cytotoxicity. Thus, to reduce the cytotoxicity of glutaraldehyde, for example, the treatment with citric acid and amino acid solutions prior to the usage and a decrease of glutaraldehyde concentration are recommended as convenient solutions [99–101].

To mimic the natural ECM, Yan *et al.* [56] prepared a rapid hydrogel by blending SF and hyaluronic acid (HA), crosslinked with carbodiimide hydrochloride (EDC) as a crosslinking agent and N-hydroxysuccinimide (NHS), 2-morpholinoethanesulfonic acid (MES) as assistant agents. HA as a component of the extracellular matrix allows small molecules to penetrate into hydrogels and exhibits good biological interactions for soft tissue regeneration applications, which is simply crosslinked via chemical agents and enzymes [102,103]. Fig. 4 shows the process of the formation of SF/HA hydrogels [56]. Here, by increasing the amount of HA, the water absorption, porosity and fracture strength of SF/HA hydrogels increased. The highest compressive strength was rendered for SF/HA hydrogel with a ratio of 6:4, measured around 207.3 kPa, while the maximum elongation at break was determined about 67.4% at a ratio of 4:6. Indeed, by increasing the amount of HA, the number of β-sheets gradually decreased and the most volume of SF/HA hydrogels contained amorphous structures. Hence, the crystallinity of the hydrogels is reduced with HA content [56].

Recently, Tavsanli *et al.* [104] synthesized a hydrogel from methacrylated hyaluronic acid (MeHA), SF and N, N-dimethyl-acrylamide (DMAA) monomer as a non-toxic spacer in aqueous solutions in the presence of an ammonium persulfate/N,N,N′,N′-tetramethylethylenediamine (APS/TEMED) redox initiator system. Here, poly(DMAA) chains were produced *in situ* and interconnected by MeHA which was crosslinked. The incorporation of SF resulted in the additional physical crosslinking due to its β-sheet domains, significantly enhancing the mechanical properties of prepared SF/HA hydrogels. Fig. 5 illustrates the schematic representation of silk-hyaluronic acid hydrogel formation using DMAA as a spacer [104].

Additionally, the change of physical or chemical conditions, such as concentration, temperature, and pH, control the gelation rate of SF solution [47,105]. Also, addition of salts, metal ions, and surfactants accelerates the conformational transition of SF aqueous solution and shortens the gelation rate [105–108].

Accordingly, Luo *et al.* [57] prepared a hydrogel composed of SF and hydroxypropyl methyl cellulose (HPMC) using simple mixing and heating. This provided compressive and tensile moduli over 1.0 MPa. Its fracture energy was up to 3.5 kJ * m^{-2}, which is higher than natural elastomers, such as cartilage and skin.

HPMC is a cellulose ether derivative with low critical solution temperature at around 62 °C and provides an hydrophobic effect due to the presence of methoxy and hydroxypropyl groups [109,110]. The structural transition of SF from random coil to β-sheet is induced by hydrophobic interaction between HPMC molecules and SF ones using heating. Indeed, small and uniform β-sheet structures form crosslinking sites entirely distributed in the hydrogel. Due to lack of biocompatible chemical agents, an SF-containing composite with appropriate mechanical properties can be safely used in tissue engineering and biomedical applications [57].

In another study, Park *et al.* [111] added methyl cellulose (MC) to SF aqueous solutions using mixing to control the gelation time of SF. Generally, MC is a hydrophilic methylated cellulose derivative obtained using chloromethane, which exhibits a unique gelation behavior due to its temperature sensitivity, as the ratio of hydrophobic molecules to hydrophilic ones in MC determines its gelation temperature [112]. Results revealed that the gelation time of SF increases with MC content. However, the compressive strength of pure SF hydrogel was 0.056 N and did not considerably change with MC content [111].

Table 2 shows a summary of the effect of enzyme, chemical and physical crosslinking of SF on its conformational transition and mechanical properties.

In another study, Das *et al.* [113] synthesized 3D bioprinted cell-laden SF-gelatin hydrogels, gelatinized using enzymatic crosslinking by mushroom tyrosinase and physical crosslinking via sonication, schematically shown in Fig. 6. Rheological properties of enzymatic and physical crosslinked SF-15 gelatin were evaluated in oscillatory mode at 18 °C, 28 °C and 37 °C. The measured storage modulus and loss modulus of enzymatic and physical crosslinked SF-15 gelatin are shown in Table 3. Accordingly, the complex modulus in the case of sonication-induced gelation exhibits a stiffer gel formation compared to tyrosinase-induced gelation, because the amounts of β-sheet which have been formed in the sonicated SF-gelatin are higher than in tyrosinase-crosslinked SF-gelatin.

5. Gamma-ray (γ-ray) irradiation

Natural and enzymatic crosslinkers, in contrast to synthetic ones,

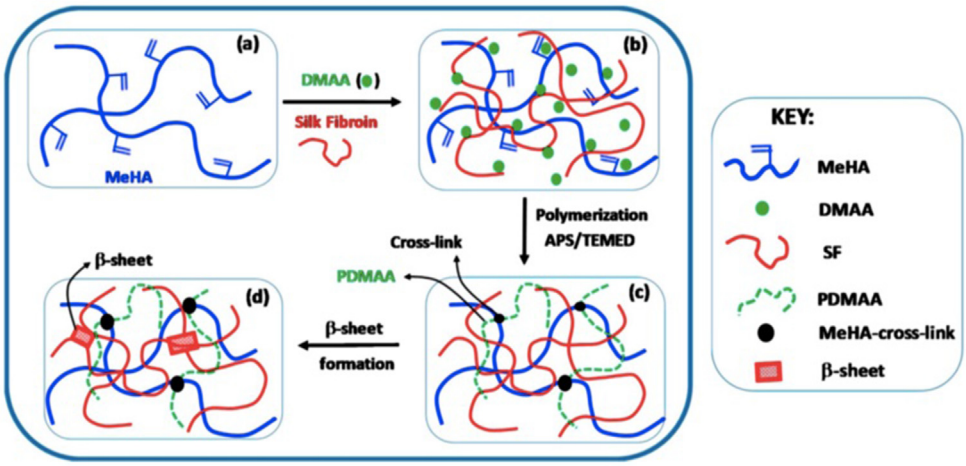

Fig. 5. The schematic representation of silk-hyaluronic acid hydrogels formation using DMAA monomer acting as a spacer. Reused with permission [104]. Copyright 2019, Elsevier.

reduce cytotoxicity. But, their application in a matrix fabrication protocol is time consuming [88]. Accordingly, researchers investigated other applicable and less harmful methods to induce hydrogelation. Radiation was investigated to prepare SF hydrogels, since chemical crosslinking and copolymerization simply occur upon irradiation to induce a hydrogel in a controllable and low cost manner without using initiators and crosslinkers [114,115]. Moreover, irradiation is often used as a sterilization method for biomedical materials in clinical applications. Among the irradiation options, gamma-rays (γ-rays) are often used for sterilization purposes, which also induces crosslinking and results in hydrogel production [116,117].

Kim *et al.* [118] synthesized SF hydrogels via a chemical crosslinking reaction using γ-ray irradiation and compared their mechanical properties with physically crosslinked SF. Compression studies revealed that in comparison with the physically crosslinked SF, the elasticity and stiffness of γ-ray irradiated SF increased, while its compressive strength decreased due to low crystallinity and intermolecular crosslinking reaction.

In another study, Xiong *et al.* [119] used γ-ray irradiation to induce the crosslinking and structural transition of SF, affecting the mechanical properties of SF films. Results showed that the strength, elongation at break and thermal decomposition temperature of SF slightly decreased by enhancing the irradiation doses, because SF molecules absorb the irradiation energy of high-energy electrons produced by γ-ray and disturb the thermodynamic equilibrium of SF. Hence, SF molecules are ionized and polarized to produce active species, resulting in splitting their hydrogen and covalent bonds [120].

On the other hand, Jin *et al.* [121] studied the effect of γ-ray on the thermo-mechanical properties of SF. Results showed that γ-ray decreased the thermo-mechanical properties of SF, and accelerated its biodegradation due to the absorption of γ-ray energy by its hydrogen and covalent bonds [122].

6. UV crosslinking of SF

Previous studies revealed that UV irradiation accelerates light aging and photo-degradation, which leads to the decrease of fiber strength. Indeed, light aging results in a photochemical reaction and formation of oxygen radicals [123,124], which attack the aromatic groups in tyrosine and phenylalanine. Such photo-degradation leads to the break of crosslinking and the brittleness of SF structure [125,126]. Photo and thermal ageing are the primary factors to estimate the life of SF under different treatment conditions due to their efficacy in increasing the amino groups content and decreasing fiber strength [127,128].

To overcome the stiff nature of SF, Maziz *et al.* [129] evaluated the chemical crosslinking of SF using light reactive acrylate groups on SF, with 2-Hydroxy-2-methylpropiophenone as a photoinitiator. SF films were then exposed to UV light through a Chrome mask for crosslinking. Here, the elongation at break and Young's modulus of non-crosslinked SF films were measured as 2.2% and 1.5 GPa, respectively. By increasing the concentration of photoinitiator from 0.2 to 1.2% w/v, the elongation at break and Young's modulus altered from 2 to 5% and 1.2 to 0.5 GPa, respectively. Indeed, the precursors and photoinitiator content affected the crosslinking density, thereby influencing the mechanical properties [73,130]. According to the structural evaluation of crosslinked films, increasing the amount of photoinitiator decreases β-sheet contents, resulting in the conformational transition of β-sheet to an amorphous structure. As a result, reducing the crystal domains enhances the elasticity of crosslinked SF films [131].

In addition, Sionkowska *et al.* [132] prepared a blend of SF and chitosan (Ch). A UV treatment at 254 nm wavelength influenced the thermal and mechanical properties of Ch/SF films. The mechanical properties of the prepared blends were significantly altered by exposing to UV irradiation. Indeed, increasing UV irradiation resulted in decreasing the elongation, ultimate tensile strength and Young's Modulus of Ch/SF films. The ultimate tensile strength and Young's Modulus of Ch/SF films with 0, 20 and 50 wt% SF were calculated as 89, 102 and 70 MPa and 0.9, 1.7 and 1.3 GPa, respectively. After 8 h of UV irradiation, the values changed as 30, 50 and 30 MPa and 0.8, 0.3 and 0.6 GPa, respectively. In order to explain these results, the viscosity of the prepared Ch/SF mixtures was measured and their optical microscopy images were investigated. The viscosity of mixtures decreased, and micro-cracks were observed on the films after UV irradiation. UV irradiation photochemically degraded both biopolymers, reduced the average molecular weight of polymers, and led to a decrease of the viscosity. Then, the reduction of the viscosity altered the secondary structure of SF. Therefore, the presence of SF in Ch/SF films results in creating the micro-cracks in the films and decreases their mechanical properties [132].

Moreover, Bessonova *et al.* [133] synthesized methacrylated silk fibroin using phenyl(2,4,6 -trimethylbenzoyl) phosphine oxide (TPO) as a photoinitiator, hexafluoroisopropanol (HFIP) as a solvent, and methacrylic anhydride as a water soluble and low cost methacrylation agent, reacting with amino groups of lysine and arginine and creating mathacrylamide functional groups. By exposing the prepared solutions to UV irradiation, the macromonomers were photocrosslinked and resulted in a strong shear modulus (G′) of 480 kPa, while G′ of pure SF was 25 kPa.

Wen *et al.* [134] prepared SF/polyvinylpyrrolidone (SF/PVP) and crosslinked using N-Vinyl-2- pyrrolidone (NVP) as a photoinitiator. The

Table 2
The effect of enzymatic, chemical and physical crosslinking on the conformational transition and mechanical properties of SF (*: the symbol > means greater than, and **: the symbol ≫ means much greater than).

Crosslinking	Crosslinker	Samples	Mechanical properties					Conformation	Ref.
			Elongation at break (%)	Elastic modulus (GPa)	Tensile strength (MPa)	Compressive strength (MPa)	Damping factor		
Enzymatic crosslinking	microbial transglutaminase (mTG) and mushroom tyrosinase	Pure SF	1.3	3.1	22.8	–	–	Silk I	[54]
		SF/gelatin (SF/G)	3.2	4.6	89.4	–	–	Silk I	
		Crosslinked SF/G	2.7–3.2	3.5–4.9	68.8–96.5	–	–	Silk I I	
	Horseradish Peroxidase (HRP) and Hydrogen Peroxide (H_2O_2)	SF nanofibers	–	10^{-6}	–	–	–	random-coil > β-sheet *	[73]
		SF nanofibers/HRP	–	$9.2–55 \times 10^{-6}$	–	–	–	β-sheet > random-coil	
		HRP-SF	–	$189.18 \pm 90.80 \times 10^{-6}$	–	–	–	β-sheet > random-coil	[45]
		ZnSr-doped β-tricalcium phosphate (HRP-SF/dTCP)	–	$226.56 \pm 60.34 \times 10^{-6}$	–	–	–	β-sheet ≫ random-coil **	
		SF-HRP (1 day after hydrogelation)	–	–	–	–	0.0121 ± 0.0004	Random coil	[82,83]
		SF-HRP (3 day after hydrogelation)	–	–	–	–	0.0208 ± 0.0042	Random coil	
		SF-HRP (7 day after hydrogelation)	–	–	–	–	0.0941 ± 0.0048	Conformational transition to β-sheet	
		SF-HRP (10 day after hydrogelation)	–	–	–	–	0.1039 ± 0.0074	β-sheet	
		SF-HRP (14 day after hydrogelation)	–	–	–	–	0.1078 ± 0.0017	β-sheet	
Chemical and physical crosslinking	Genipin	chitosan/silk fibroin	–	$\ll 578.6 \pm 28.8 \times 10^{-6}$	–	–	–	α-helix/random-coil	[71]
		chitosan/silk fibroin/ 20genipin	–	$578.6 \pm 28.8 \times 10^{-6}$	–	–	–	β-sheet	
	Glutaraldehyde	SF film	4.53	–	15.6	–	–	α-helix and 33.2% β-sheet	[89]
		SF/7.5glutaraldehyde	9.97	–	21.8	–	–	β-sheet ≫α-helix	
		SF	~20	$\sim 270 \times 10^{-3}$	~11	–	–	34% β-sheet	[55]
		SF/30gelatin	~15	$\sim 350 \times 10^{-3}$	~14	–	–	43% β-sheet	
	carbodiimide hydrochloride (EDC)	SF/20hyaluronic acid	–	–	–	91.1×10^{-3}	–	random-coil > β-sheet	[56]
		SF/40hyaluronic acid	–	–	–	207.3×10^{-3}	–	β-sheet ≫ random-coil	
		SF/60hyaluronic acid	–	–	–	$\sim 120 \times 10^{-3}$	–	β-sheet > random-coil	
	N, N-dimethyla- crylamide (DMAA)	SF/hyaluronic acid + 4DMAA	–	$54 \pm 5 \times 10^{-6}$	–	–	–	~30% β-sheet	[104]
		SF/hyaluronic acid + 25DMAA	–	$99 \pm 11 \times 10^{-6}$	–	–	–	60–70% β-sheet	
	Mixing ratio	SF/50hydroxypropyl methyl cellulose (HPMC)	–	–	–	~0.05	–	< 63.8% β-sheet	[57]
		SF/90HPMC	–	–	–	~0.65	–	63.8% β-sheet	
	Heating	SF (37 °C)	–	–	–	~0.03 N	–	random-coil > β-sheet	
		SF (50 °C)	–	–	–	~0.55 N	–	β-sheet > random-coil	

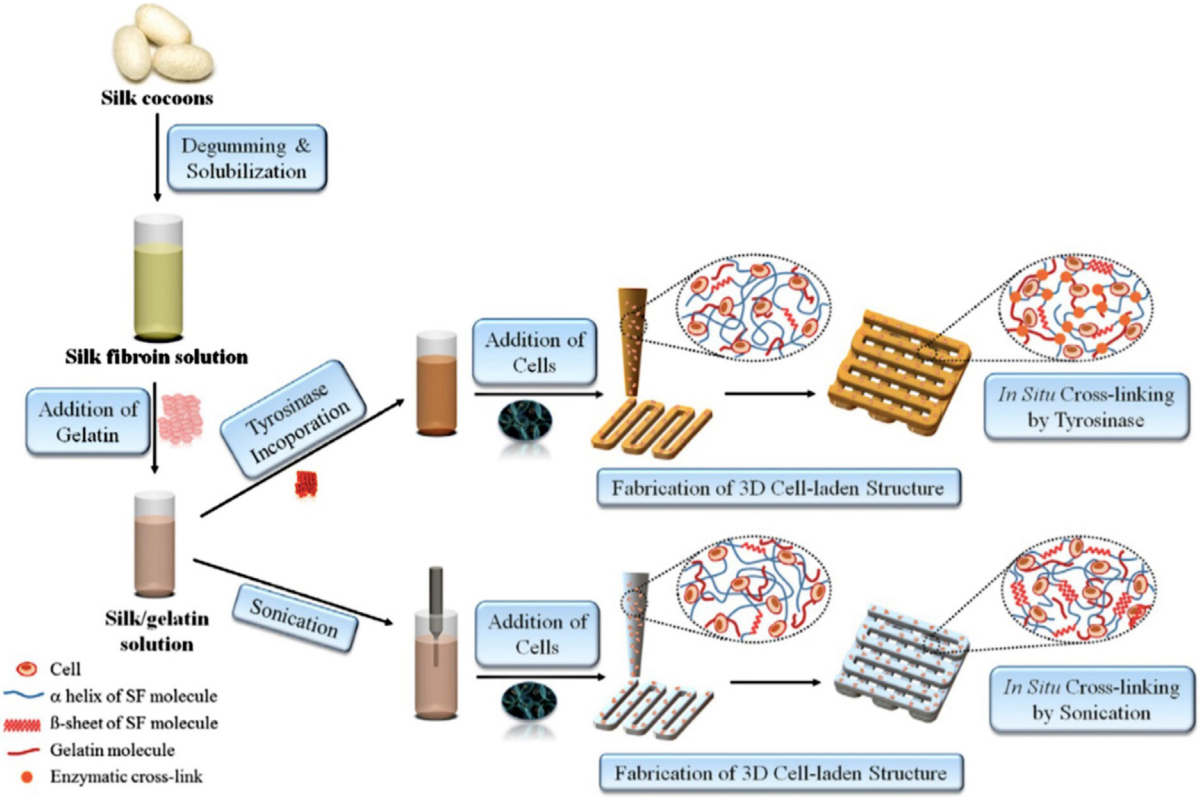

Fig. 6. The schematic representation of preparing bioprinted cell-laden SF-gelatin hydrogels using enzymatic and physical crosslinking. Reused with permission [113]. Copyright 2015, Elsevier.

Table 3
Storage modulus and loss modulus of SF-gelatin hydrogels crosslinked via mushroom tyrosinase and sonication [113].

Samples	Storage modulus (Pa)			Loss modulus (Pa)		
	18 °C	28 °C	37 °C	18 °C	28 °C	37 °C
SF-gelatin- Tyrosinase	530,000	415,000	166,000	58,700	65,900	31,300
SF-gelatin- Sonication	751,000	504,000	221,000	84,500	32,800	42,200

evaluation of mechanical properties of SF/PVP samples with various ratios of SF/NVP, after 30 min of exposing to UV-irradiation, revealed that the lowest and highest compressive strength of SF/PVP were determined 20.04 kPa and 60.9 kPa, provided by SF/NVP ratios of 5:5 and 8:2, respectively. Because, UV irradiation causes the formation of some O_3 which changed into free radicals, resulting in the polymerization of NVP, then polymerized NVP leads to entangle PVP with dityrosine of SF [73,135].

7. Photo crosslinking of SF

To provide a biologically and environmentally friendly crosslinking technique, Applegate *et al.* [136] crosslinked SF by riboflavin and exposed it to visible light due to strong light absorbance of riboflavin in the range of 330 to 470 nm. Previous researches had used riboflavin as a photo crosslinker for collagen [137], alginate [138], and polyethylene glycol [139]. Applegate *et al.* [136] demonstrated that by increasing the period of light exposure of SF/riboflavin samples from 0 min to 50 min, the shear modulus increased modestly from 40 Pa to 47 Pa. Visible light excites riboflavin and radicalizes tyrosine residues of SF, leading to the formation of dityrosine complexes, bonding SF chains.

Table 4 shows a summary of the effect of different irradiations on the conformational transition and mechanical properties of SF.

8. Sterilization methods

Different methods have been used for the sterilization of biomaterials, such as steam, gamma radiation and ethylene oxide [140–142]. The best sterilization method focuses on the effect of both removing of microorganisms and improving mechanical properties of the applied biomaterial [143]. Accordingly, Zhao *et al.* [144] investigated the effect of different doses and exposure time of these three aforementioned sterilization methods on the molecular structure and mechanical properties of SF. The mechanical experiments illustrated that the fracture strength of the unsterilized SF, sterilized SF using steam, gamma irradiation and ethylene were 4.3, 2.9, 4.2 and 4.0 N, respectively. In addition, the results did not show a significant difference between the strength of the samples sterilized using gamma irradiation and ethylene oxide sterilization, while SF samples sterilized using steam exhibits various behaviors. The high temperature, humidity and pressure of steam resulted in hydrolysis of the polymer with increasing the exposure time of sterilization [145], leading to a decrease in the molecular weight of SF and an increase in β-sheets conformation. This consequently resulted in decreasing the mechanical properties of SF. However, γ-ray irradiation caused a significant degradation in the amorphous region of SF and slightly decreased its molecular weight. Further, ethylene oxide did not react with the functional groups of SF samples nor changed their structures. Therefore, ethylene oxide seems the best sterilizing agent for SF [144].

9. Water treatment

As mentioned above, SF is mainly composed of β-sheet crystalline domains and amorphous regions. Therefore, the strength of SF considerably depends on the integrity of the SF structure. As a solvent, water influences the structure and strength of SF [146,147]. The initial studies on SF were mostly focused on the effects of moisture on the

Table 4
The effect of irradiation on the conformational transition and mechanical properties of SF (*: the symbol > means greater than).

Crosslinking	Crosslinker	Samples	Mechanical properties				Conformation	Ref.
			Elongation at break (%)	Elastic modulus (GPa)	Tensile strength (MPa)	Compressive strength (MPa)		
γ-ray irradiation	γ-ray	SF	–	–	–	~0.001	silk I and silk II	[118]
		γ-ray irradiated SF	–	–	–	~0.008	silk I and silk II	
		SF	~2.5	–	~50	–	silk I and silk II	[119]
		SF (50 kGy)	~2.0	–	~38	–	silk I and silk II	
		SF (100 kGy)	~1.7	–	~30	–	silk I and silk II	
		SF (200 kGy)	~1.2	–	~20	–	silk I and silk II	
		SF	~5.5	–	~50 N	–	γ-ray decreases the thermo-mechanical properties of	[121]
		SF (25 kGy)	~3.7	–	~45 N	–	SF, and accelerates its biodegradation due to the	
		SF (50 kGy)	~3.1	–	~43 N	–	absorption of γ-ray energy by its hydrogen and	
		SF (100 kGy)	~3.0	–	~38 N	–	covalent bonds	
		SF (200 kGy)	~2.6	–	~29 N	–		
		SF (300 kGy)	~2.5	–	~25 N	–		
		SF (500 kGy)	~2.1	–	~3 N	–		
		SF (1000 kGy)	~1.9	–	~2 N	–		
UV irradiation	UV	SF	2.2	1.5	~40	–	β-sheet contents decrease by increasing the	[129]
		SF/0.2Photoinitiator	2.0	1.2	~15	–	photoinitiator concentration	
		SF/0.4Photoinitiator	2.8	1.05	~18	–		
		SF/0.6Photoinitiator	3.4	0.86	~23	–		
		SF/0.8Photoinitiator	4.5	0.87	~30	–		
		SF/1.2Photoinitiator	5	0.50	~16	–		
		Chitosan/50SF (4 h UV)	–	2.0 ± 0.10	53 ± 2.6	–	Silk fibroin results in a fragile structure in blends	[132]
		Chitosan/20SF (4 h UV)	–	0.5 ± 0.02	70 ± 3.5	–		
		Chitosan (4 h UV)	–	0.6 ± 0.03	73 ± 3.6	–		
		Chitosan/20SF (0 h UV)	–	1.3 ± 0.06	102 ± 5.1	–	UV-irradiation causes the photochemical degradation	[132]
		Chitosan/20SF (4 h UV)	–	0.5 ± 0.02	70 ± 3.5	–	of both biopolymers, resulting in the viscosity	
		Chitosan/20SF (8 h UV)	–	0.3 ± 0.01	50 ± 2.5	–	reduction	
		SF	–	25×10^{-6}	–	–	Random coil	[133]
		SF/ethacrylic anhydride dissolved in formic acid (10 min UV and photoinitiator: diphenyl(2,4,6-trimethylbenzoyl)phosphine oxide (TPO))	–	120×10^{-6}	–	–	antiparallel β-sheets	
		SF/ethacrylic anhydride dissolved in hexafluoroisopropanol (10 min UV and photoinitiator: diphenyl(2,4,6-trimethylbenzoyl)phosphine oxide (TPO))	–	480×10^{-6}	–	–	Additional covalent cross-links and antiparallel β-sheets	
		SF/PVP	–	–	–	9.94×10^{-3}	Random coil > β-sheets *	[134]
		SF/30PVP (10NVP and 30 min UV)	–		–	55.30×10^{-3}	β-sheet formation	
		SF/30PVP (20NVP and 30 min UV)	–	–	–	60.90×10^{-3}	It is 100% light transmitting and can completely photocrosslinked.	
		SF/30PVP (30NVP and 30 min UV)	–	–	–	37.85×10^{-3}	Due to the formation of IPN, the crosslinking limits	
		SF/30PVP (40NVP and 30 min UV)	–	–	–	26.68×10^{-3}	the self-assembly of SF chains. Then, SF chains cannot	
		SF/30PVP (50NVP and 30 min UV)	–	–	–	20.04×10^{-3}	rotate freely to achieve a stable β-sheet structure.	
Visible light irradiation	Visible light	SF/riboflavin	–	40×10^{-9}	–	–	The formation of dityrosine complexes by exciting	[136]
		SF/riboflavin (50 min exposed by visible light)	–	47×10^{-9}	–	–	riboflavin via visible light	

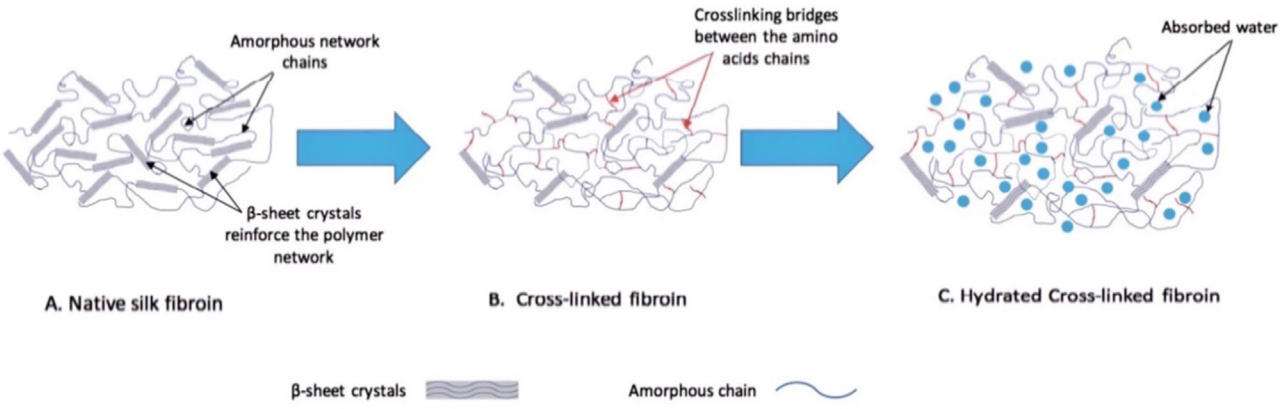

Fig. 7. The schematic illustrations of the changes of SF structure after chemical crosslinking and water absorption. Reused with permission [129]. Copyright 2018, IOP Publishing.

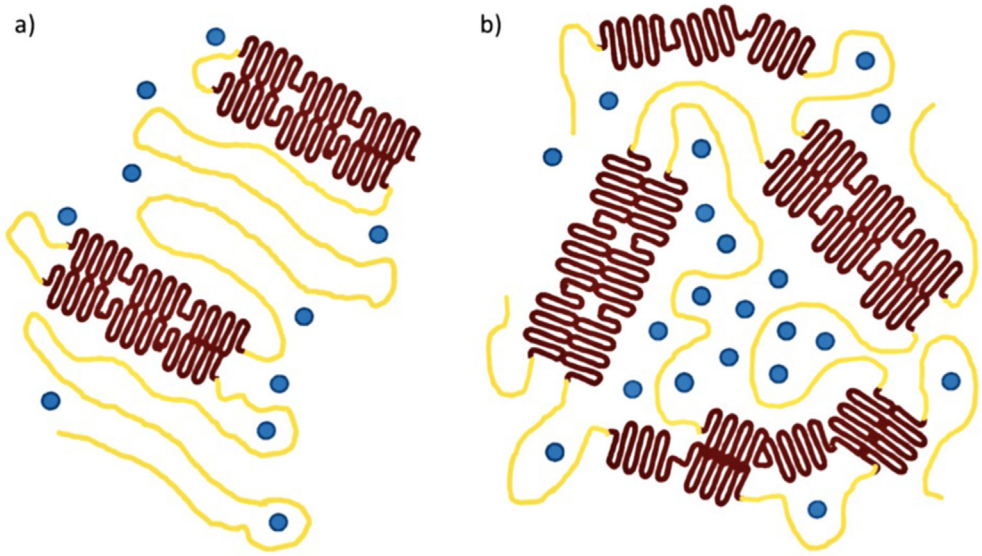

Fig. 8. The schematic drawing of SF secondary structure for both (a) water annealed and (b) methanol immersed SF in which amorphous, β-sheet crystalline regions, and water molecules are displayed via yellow, brown and blue colors, respectively. Reused with permission [159]. Copyright 2010, Wiley. (For interpretation of the references to colour in this figure legend, the reader is referred to the web version of this article.)

amorphous domains of SF schematically exhibited in Fig. 7 [129,147], while recent studies are considering the effects of moisture on the β-sheet structure of SF and its strength. Accordingly, Cheng *et al.* [148] found that water reduces the hydrogen bonds between β-sheets in SF, hence significantly decreasing its strength. Indeed, via an in-depth investigation of the functional groups and structure of SF in presence of water solvent, they found that water molecules prevent the formation of hydrogen bonds between β-sheets in the crystalline regions. Therefore, the resultant structure of SF becomes weak and brittle, thus decreasing the ultimate tensile strength.

The hydrophobic crystalline β-sheet domains are incorporated into the hydrophilic amorphous regions, containing moisture. Polypeptide chains composed of the amino acids, such as glycine and alanine, grafted together by strong hydrogen bonds, make the main components of the crystalline β-sheets [149,150]. The amorphous domains significantly impact the soft matrix of SF due to their disordered structure, while the strength of SF structure is derived by the crystalline β-sheet domains [151,152].

Huang *et al.* [153] prepared SF mats using electrospinning, then annealed by mild water vapor at different annealing times and temperatures to improve the mechanical properties. Generally, various treatments exist to improve the mechanical properties of the prepared SF samples. Most of the treatment methods require chemical agents, such as alcoholic solutions [154], which may negatively affect the normal physiologic functions when directly applied to humans or affect the pharmacodynamics or pharmacokinetics of drugs when used in drug delivery systems [155]. Accordingly, Min *et al.* [156] used water vapor annealing as a safe treatment method to induce the conformational transition in SF. However, the treating time and the temperature are the most important factors to determine the extent of the structural transition [157]. Hence, Huang *et al.* [153] confirmed that water vapor can induce the conformational transition of SF from random coil to β-sheet and improve the mechanical properties of SF mats. Here, the fracture strength of SF mats alters irregularly with annealing time and temperature. Indeed, by simultaneously increasing the annealing time and temperature up to 15 h and 65 °C, respectively, the fracture strength increased, while by further rising both time and temperature, the strength decreased. However, the resultant strength of SF mats obtained after water vapor treatment was significantly lower than that of post-treated samples via ethanol solution [158].

In another study, Lawrence *et al.* [159] investigated the efficacy of hydration on SF structure using water annealing and methanol treatment. Here, the content of β-sheets through methanol treatment increased more than during water annealing due to the increase of film thickness by swelling in methanol. In dry state, the greater content of β-sheets increases the stiffness of SF. Conversely, the water absorption in hydrated state results in enhancing the ductility of SF.

Yazawa *et al.* [160] investigated the influence of water content on β-sheet formation and mechanical properties of SF. The tensile properties of SF were evaluated at different relative humidities (RH). The tensile

Table 5
The effect of sterilization, water and alcoholic treatments on the conformational transition and mechanical properties of SF.

Crosslinking	Samples	Mechanical properties				Conformation	Ref.
		Elongation at break (%)	Elastic modulus (GPa)	Tensile strength (MPa)	Compressive strength (MPa)		
Sterilization methods	SF	–	–	4.3 N	–		[144]
	SF sterilized via steam	–	–	2.9 N	–	The steam hydrolyzes the polymer, leading to a decrease in the molecular weight of SF.	
	SF sterilized via γ-ray	–	–	4.2 N	–	γ-ray does not significantly change SF structure.	
	SF sterilized via Ethylene oxide	–	–	4.0 N	–	Ethylene oxide did not react with SF functional groups nor changed their structures.	
Water treatment	SF	–	–	~1.2	–	Silk I	[153]
	SF (5 h in water vapor 65 °C)	–	–	~5.6	–	Silk I to silk II	
	SF (10 h in water vapor 65 °C)	–	–	~5.8	–	Silk I to silk II	
	SF (15 h in water vapor 65 °C)	–	–	~6.1	–	Silk I to silk II	
	SF (25 h in water vapor 65 °C)	–	–	~6.4	–	Silk I to silk II	
	SF (3 h in water vapor 45 °C)	–	–	~3.9	–	Silk I to silk II	
	SF (3 h in water vapor 55 °C)	–	–	~4.2	–	Silk I to silk II	
	SF (3 h in water vapor 65 °C)	–	–	~~5.3	–	Silk I to silk II	
	SF (3 h in water vapor 75 °C)	–	–	~6.0	–	Silk I to silk II	
	SF mat	7.6 ± 1.7	$17.7 \pm 6.8 \times 10^{-3}$		–	Random coil	[156]
	SF mat-water vapor treated	8.5 ± 2.0	$30.4 \pm 4.4 \times 10^{-3}$	–	–	the changes in the hydrogen bonding and β-sheet formation	
	SF mat-Methanol treated	4.4 ± 0.7	$104.3 \pm 13.7 \times 10^{-3}$	–	–	β-sheet formation	
	SF film-5 h water vapor treated	136 ± 48	$21.97 \pm 1.52 \times 10^{-3}$	3.61 ± 0.75	–	β-sheet	[159]
	SF film-20 min Methanol treated	149 ± 45	$18.70 \pm 6.98 \times 10^{-3}$	4.02 ± 0.97	–	β-sheet	
Alcoholic treatment	SF-45 min Methanol treated	–	$\sim 0.1 \times 10^{-3}$	–	~0.5	Random coil	[165]
	SF/10hyaluronic acid-45 min Methanol treated	–	$\sim 0.7 \times 10^{-3}$	–	~2.1	β-sheet formation	
	SF/20hyaluronic acid-45 min Methanol treated	–	$\sim 2.0 \times 10^{-3}$	–	~3.1	β-sheet formation	
	SF/40hyaluronic acid-45 min Methanol treated	–	$\sim 5.7 \times 10^{-3}$	–	~8.0	β-sheet	
	SF-45 min Methanol treated-8 weeks water washed	–	$\sim 0.2 \times 10^{-3}$	–	~0.5	Random coil	
	SF/10hyaluronic acid-45 min Methanol treated-8 weeks water washed	–	$\sim 0.3 \times 10^{-3}$	–	~1.9	β-sheet formation	
	SF/20hyaluronic acid-45 min Methanol treated-8 weeks water washed	–	$\sim 0.4 \times 10^{-3}$	–	~2.5	β-sheet formation	
	SF/40hyaluronic acid-45 min Methanol treated-8 weeks water washed	–	$\sim 1.0 \times 10^{-3}$	–	~4.1	β-sheet formation	
	SF mat	21.7 ± 4.3	$253 \pm 31 \times 10^{-3}$	–	–	Random coil	
	SF mat-5 min ethanol treated	19.1 ± 4	$231 \pm 32 \times 10^{-3}$	–	–	β-sheet formation	
	SF mat-20 min ethanol treated	13.2 ± 2.8	$170 \pm 40 \times 10^{-3}$	–	–	β-sheet formation	
	SF mat-60 min ethanol treated	11.9 ± 3.1	$140 \pm 39 \times 10^{-3}$	–	–	β-sheet formation	
	SF mat-24 h ethanol treated	12.2 ± 2.5	$490 \pm 70 \times 10^{-3}$	–	–	55.27% β-sheet	
	SF mat-5 min methanol treated	16.8 ± 2.8	$170 \pm 35 \times 10^{-3}$	–	–	β-sheet formation	
	SF mat-20 min methanol treated	15.9 ± 1.48	$350 \pm 52 \times 10^{-3}$	–	–	β-sheet formation	
	SF mat-60 min methanol treated	11.8 ± 3.3	$213 \pm 28 \times 10^{-3}$	–	–	β-sheet formation	
	SF mat-24 h methanol treated	8.2 ± 2.8	$610 \pm 46 \times 10^{-3}$	–	–	53% β-sheet	
	SF ultrathin film-methanol treated	0.5	8.6 ± 2.1	100	–	β-sheet	[170]
	SF ultrathin film-water treated	0.3	3.4 ± 1.5	100	–	β-sheet formation	

strength, Young's modulus, elongation at break and toughness of SF films did not significantly change up to RH 84%. However, the elongation at break and toughness of SF films incubated at RH 97% enhanced 15 and 17 times higher than those incubated at RH 84%, respectively. The crystallinity content of SF films increased up to 30% for samples incubated at RH from 6% to 75%, while the crystallinity increased to approximately 40% at over RH 84%. Because, water molecules induce β-sheet formation via helix-helix interactions. Therefore, at RH 97%, amorphous regions of SF were plasticized via water molecules and its elasticity increased. Indeed, bound water disrupts the intermolecular cohesive forces between protein chains, leading to increase the steric hindrance which enhances the chain movements in amorphous regions and induces β-sheet crystallization in SF.

10. Alcohol treatment

As mentioned previously, the conformational transition of SF is an important parameter which affects its physical and chemical properties. The process factors, such as concentration, solvent and drying temperature can modify the conformation of SF [161]. Alongside these factors, treatments can affect the structural transition of SF from random coil to β-sheet. Low dielectric organic materials, such as methanol, ethanol or dioxane are general solvents to control the conformational transition of SF and to decrease its water solubility [162–164].

Garcia-Fuentes *et al.* [165] investigated the molecular conformation of SF in SF/Hyaluronic acid (SF/HA) mixture post-treated in methanol and water. Structural studies illustrated that the conformational transition of SF from random coil to β-sheet considerably arose in methanol incubated SF/HA samples and improved their mechanical properties, while HA induced the structural transition of SF into a less crystalline β-sheet structure when incubated in water [165]. Fig. 8 shows the schematic drawing of SF secondary structure for both water annealed and methanol immersed SF [159].

In addition, Amiraliyan *et al.* [166] synthesized electrospun SF mats post-treated with methanol and ethanol to improve their mechanical properties. The experimental results showed that both methanol and ethanol treatments increased the tensile strength of SF mats, while the elongation at break reduced. Indeed, alcohol as a polar media absorbs water from SF molecules and enhances hydrophobic amino acids, such as Alanine and Glycine, thus resulting in enhancing the crystalline domains and inducing β-sheet formations [167–169].

Furthermore, Jiang *et al.* [170] fabricated SF layer-by-layer films with and without methanol treatment. The mechanical evaluations revealed that both tensile and compression strengths were enhanced in methanol treated SF films and the ultimate tensile strength and elastic modulus attained were up to 100 MPa and 8.6 ± 2.1 GPa, respectively. This was due to the increase in crystalline β-sheets as the reinforcing fillers and the formation of a network of physical crosslinks, after methanol treatment [170,171].

Table 5 shows the effect of sterilization, water and alcoholic treatments on the conformational transition and mechanical properties of SF.

11. Summary and outlook

Silk fibroin has been widely used as a biomaterial for biomedical applications due to its superior host response, gradual biodegradability and specific mechanical properties. Hence, various researches have tightly focused on enhancing the mechanical properties of SF by different techniques without negatively affecting its biological properties. Among these techniques, a treatment is an effective method, employed as the step of the processing and plays a significant role in improving the mechanical properties of SF. In the present review, the typical treatment methods of SF involving enzymatic, chemical and physical crosslinking, UV, γ-ray and visible light irradiation, sterilization methods, and the effect of water and alcohol on SF structure and its resulting mechanical properties were summarized. Numerous studies demonstrated that most of the treatment methods change the random coil structure of SF to β-sheet conformation and improve the mechanical properties of SF. In addition to the mechanical properties, the safety and biological friendliness of some of the utilized treating materials was discussed. Moreover, the mechanism of treating methods has been briefly discussed to evaluate the molecular behavior of SF under the influence of each treatment materials and techniques. Accordingly, in the future, treated SF with desirable mechanical properties and exceptional host response could be applicable for tissue engineering and regenerative medicine.

In the present review, the effect of treatment methods on SF conformational transition and mechanical properties was investigated mainly for samples prepared in pure state of SF, while these effects and outcomes can be comprehensively challenged and elaborated in detail for the blended SF with other natural and synthetic hydrogels. Furthermore, numerous studies have assayed the tensile, compressive and rheological properties of SF hydrogels as conventional testing, while the small scale is an issue for evaluating the mechanical properties of heterogeneous tissues and small biological devices prepared via hydrogels. Therefore, nanoindentation and unconfined compression tests can be performed as exceptional methods for probing the mechanical properties of small scale biological devices and hydrogels swelling behavior.

Declaration of Competing Interest

The authors declare that they have no known competing financial interests or personal relationships that could have appeared to influence the work reported in this paper.

Acknowledgements

Lorenzo Moroni is grateful to the European Research Council starting grant "Cell Hybridge" (Grant #637308). We also acknowledge support from the Dutch Province of Limburg.

Appendix A. Supplementary material

Supplementary data to this article can be found online at https://doi.org/10.1016/j.eurpolymj.2020.109842.

References

[1] F.M. Watt, W.T. Huck, Role of the extracellular matrix in regulating stem cell fate, Nat. Rev. Mol. Cell Biol. 14 (8) (2013) 467.
[2] F.M. Watt, H. Fujiwara, Cell-extracellular matrix interactions in normal and diseased skin, Cold Spring Harbor Perspect. Biol. 3 (4) (2011) a005124.
[3] D. Seliktar, Designing cell-compatible hydrogels for biomedical applications, Science 336 (6085) (2012) 1124–1128.
[4] A. Shakoor, R. Muhammad, N. Thomas, V. Silberschmidt, Mechanical and thermal characterisation of poly (l-lactide) composites reinforced with hemp fibres, Journal of Physics: Conference Series, IOP Publishing, 2013, p. 012010.
[5] A.J. Engler, S. Sen, H.L. Sweeney, D.E.J.C. Discher, Matrix elasticity directs stem cell lineage specification, 126(4) (2006) 677–689.
[6] S. Bai, H. Han, X. Huang, W. Xu, D.L. Kaplan, H. Zhu, Q. Lu, Silk scaffolds with tunable mechanical capability for cell differentiation, Acta Biomater. 20 (2015) 22–31.
[7] G. Abagnale, M. Steger, V.H. Nguyen, N. Hersch, A. Sechi, S. Joussen, B. Denecke, R. Merkel, B. Hoffmann, A. Dreser, Surface topography enhances differentiation of mesenchymal stem cells towards osteogenic and adipogenic lineages, Biomaterials 61 (2015) 316–326.
[8] H. Liu, M. Li, S. Liu, P. Jia, X. Guo, S. Feng, T.J. Lu, H. Yang, F. Li, F. Xu, Spatially modulated stiffness on hydrogels for soft and stretchable integrated electronics, Mater. Horiz. (2019).
[9] A.J. Engler, S. Sen, H.L. Sweeney, D.E. Discher, Matrix elasticity directs stem cell lineage specification, Cell 126 (4) (2006) 677–689.
[10] J.S. Park, J.S. Chu, A.D. Tsou, R. Diop, Z. Tang, A. Wang, S. Li, The effect of matrix stiffness on the differentiation of mesenchymal stem cells in response to TGF-β, Biomaterials 32 (16) (2011) 3921–3930.

[11] R. Narayanaswamy, V.P. Torchilin, Hydrogels and their applications in targeted drug delivery, Molecules 24 (3) (2019) 603.
[12] V. Pérez-Luna, O. González-Reynoso, Encapsulation of biological agents in hydrogels for therapeutic applications, Gels 4 (3) (2018) 61.
[13] R. Moreddu, D. Vigolo, A.K. Yetisen, Contact lens technology: from fundamentals to applications, Adv. Healthcare Mater. (2019) 1900368.
[14] J.-H. Lee, H.-W. Kim, Emerging properties of hydrogels in tissue engineering, J. Tissue Eng. Regenerative Med. 9 (2018) 2041731418768285.
[15] G. Kaur, F. Baino, J.C. Mauro, V. Kumar, G. Pickrell, N. Sriranganathan, S.G. Waldrop, Biomaterials for Cell Encapsulation: Progress Toward Clinical Applications, Clinical Applications of Biomaterials, Springer, 2017, pp. 425–458.
[16] D.F. Williams, There is no such thing as a biocompatible material, Biomaterials 35 (38) (2014) 10009–10014.
[17] S. Garg, A. Garg, Hydrogel: classification, properties, preparation and technical features, Asian J. Biomat. Res 2 (2016) 163–170.
[18] M. Bahram, N. Mohseni, M. Moghtader, An introduction to hydrogels and some recent applications, Emerging concepts in analysis and applications of hydrogels, IntechOpen; 2016.
[19] Q. Chai, Y. Jiao, X. Yu, Hydrogels for biomedical applications: their characteristics and the mechanisms behind them, Gels 3 (1) (2017) 6.
[20] Z. Shi, X. Gao, M.W. Ullah, S. Li, Q. Wang, G. Yang, Electroconductive natural polymer-based hydrogels, Biomaterials 111 (2016) 40–54.
[21] J. Zhu, R.E. Marchant, Design properties of hydrogel tissue-engineering scaffolds, Expert Rev. Med. Devices 8 (5) (2011) 607–626.
[22] M.C. Catoira, L. Fusaro, D. Di Francesco, M. Ramella, F. Boccafoschi, Overview of natural hydrogels for regenerative medicine applications, J. Mater. Sci. - Mater. Med. 30 (10) (2019) 115.
[23] J.P. Gong, Y. Katsuyama, T. Kurokawa, Y. Osada, Double-network hydrogels with extremely high mechanical strength, Adv. Mater. 15 (14) (2003) 1155–1158.
[24] J.P. Gong, Why are double network hydrogels so tough? Soft Matter 6 (12) (2010) 2583–2590.
[25] E.M. Ahmed, Hydrogel: Preparation, characterization, and applications: A review, J. Adv. Res. 6 (2) (2015) 105–121.
[26] S. Van Vlierberghe, P. Dubruel, E. Schacht, Biopolymer-based hydrogels as scaffolds for tissue engineering applications: a review, Biomacromolecules 12 (5) (2011) 1387–1408.
[27] A.M. Jonker, D.W. Löwik, J.C. van Hest, Peptide-and protein-based hydrogels, Chem. Mater. 24 (5) (2012) 759–773.
[28] S.H. Lee, Y. Lee, S.-W. Lee, H.-Y. Ji, J.-H. Lee, D.S. Lee, T.G. Park, Enzyme-mediated cross-linking of Pluronic copolymer micelles for injectable and in situ forming hydrogels, Acta Biomater. 7 (4) (2011) 1468–1476.
[29] W. Hu, Z. Wang, Y. Xiao, S. Zhang, J. Wang, Advances in crosslinking strategies of biomedical hydrogels, Biomater. Sci. 7 (3) (2019) 843–855.
[30] H.K. Lau, K.L. Kiick, Opportunities for multicomponent hybrid hydrogels in biomedical applications, Biomacromolecules 16 (1) (2014) 28–42.
[31] B. Balakrishnan, R. Banerjee, Biopolymer-based hydrogels for cartilage tissue engineering, Chem. Rev. 111 (8) (2011) 4453–4474.
[32] S. Das, M. Sharma, D. Saharia, K.K. Sarma, E.M. Muir, U. Bora, Electrospun silk-polyaniline conduits for functional nerve regeneration in rat sciatic nerve injury model, Biomed. Mater. 12 (4) (2017) 045025.
[33] D. Naskar, A.K. Ghosh, M. Mandal, P. Das, S.K. Nandi, S.C. Kundu, Dual growth factor loaded nonmulberry silk fibroin/carbon nanofiber composite 3D scaffolds for in vitro and in vivo bone regeneration, Biomaterials 136 (2017) 67–85.
[34] E. Ko, J.S. Lee, H. Kim, S.Y. Yang, D. Yang, K. Yang, J. Lee, J. Shin, H.S. Yang, W. Ryu, Electrospun silk fibroin nanofibrous scaffolds with two-stage hydroxyapatite functionalization for enhancing the osteogenic differentiation of human adipose-derived mesenchymal stem cells, ACS Appl. Mater. Interfaces 10 (9) (2017) 7614–7625.
[35] W. Shi, M. Sun, X. Hu, B. Ren, J. Cheng, C. Li, X. Duan, X. Fu, J. Zhang, H. Chen, Structurally and functionally optimized silk-fibroin–gelatin scaffold using 3D printing to repair cartilage injury in vitro and in vivo, Adv. Mater. 29 (29) (2017) 1701089.
[36] S.-Y. Xie, L.-H. Peng, Y.-H. Shan, J. Niu, J. Xiong, J.-Q. Gao, Adult stem cells seeded on electrospinning silk fibroin nanofiberous scaffold enhance wound repair and regeneration, J. Nanosci. Nanotechnol. 16 (6) (2016) 5498–5505.
[37] C. Xue, H. Zhu, D. Tan, H. Ren, X. Gu, Y. Zhao, P. Zhang, Z. Sun, Y. Yang, J. Gu, Electrospun silk fibroin-based neural scaffold for bridging a long sciatic nerve gap in dogs, J. Tissue Eng. Regenerative Med. 12 (2) (2018) e1143–e1153.
[38] K. Zhan, L. Bai, Q. Wu, D. Lei, G. Wang, Fractal characteristics of the microvascular network: a useful index to assess vascularization level of porous silk fibroin biomaterial, J. Biomed. Mater. Res. Part A 105 (8) (2017) 2276–2290.
[39] D.B. Khadka, D.T. Haynie, Protein-and peptide-based electrospun nanofibers in medical biomaterials, Nanomedicine: Nanotechnology, Biol. Med. 8 (8) (2012) 1242–1262.
[40] Y. Wang, X. Wang, J. Shi, R. Zhu, J. Zhang, Z. Zhang, D. Ma, Y. Hou, F. Lin, J. Yang, A biomimetic silk fibroin/sodium alginate composite scaffold for soft tissue engineering, Sci. Rep. 6 (2016) 39477.
[41] M.S. Zafar, D.J. Belton, B. Hanby, D.L. Kaplan, C.C. Perry, Functional material features of Bombyx mori silk light versus heavy chain proteins, Biomacromolecules 16 (2) (2015) 606–614.
[42] Y. Qi, H. Wang, K. Wei, Y. Yang, R.-Y. Zheng, I. Kim, K.-Q. Zhang, A review of structure construction of silk fibroin biomaterials from single structures to multi-level structures, Int. J. Mol. Sci. 18 (3) (2017) 237.
[43] B. Kundu, R. Rajkhowa, S.C. Kundu, X. Wang, Silk fibroin biomaterials for tissue regenerations, Adv. Drug Deliv. Rev. 65 (4) (2013) 457–470.
[44] J.L. Whittaker, N.R. Choudhury, N.K. Dutta, A. Zannettino, Facile and rapid ruthenium mediated photo-crosslinking of Bombyx mori silk fibroin, J. Mater. Chem. B 2 (37) (2014) 6259–6270.
[45] V.P. Ribeiro, S. Pina, J.B. Costa, I.F. Cengiz, L. García-Fernández, M.d.M. Fernández-Gutiérrez, O.C. Paiva, A.L. Oliveira, J. San-Román, J.M. Oliveira, Enzymatically cross-linked silk fibroin-based hierarchical scaffolds for osteochondral regeneration, ACS Appl. Mater. Interfaces 11 (4) (2019) 3781–3799.
[46] Y. Lin, X. Xia, K. Shang, R. Elia, W. Huang, P. Cebe, G. Leisk, F. Omenetto, D.L. Kaplan, Tuning chemical and physical cross-links in silk electrogels for morphological analysis and mechanical reinforcement, Biomacromolecules 14 (8) (2013) 2629–2635.
[47] A. Matsumoto, J. Chen, A.L. Collette, U.-J. Kim, G.H. Altman, P. Cebe, D.L. Kaplan, Mechanisms of silk fibroin sol − gel transitions, J. Phys. Chem. B 110 (43) (2006) 21630–21638.
[48] T. Yucel, P. Cebe, D.L. Kaplan, Vortex-induced injectable silk fibroin hydrogels, Biophys. J. 97 (7) (2009) 2044–2050.
[49] W. Xiao, W. Liu, J. Sun, X. Dan, D. Wei, H. Fan, Ultrasonication and genipin cross-linking to prepare novel silk fibroin–gelatin composite hydrogel, J. Bioactive Compatible Polym. 27 (4) (2012) 327–341.
[50] E.S. Gil, R.J. Spontak, S.M. Hudson, Effect of β-sheet crystals on the thermal and rheological behavior of protein-based hydrogels derived from gelatin and silk fibroin, Macromol. Biosci. 5 (8) (2005) 702–709.
[51] M. Stoppato, H.Y. Stevens, E. Carletti, C. Migliaresi, A. Motta, R.E. Guldberg, Effects of silk fibroin fiber incorporation on mechanical properties, endothelial cell colonization and vascularization of PDLLA scaffolds, Biomaterials 34 (19) (2013) 4573–4581.
[52] Y.H. Na, Double network hydrogels with extremely high toughness and their applications, Korea-Australia Rheol. J. 25 (4) (2013) 185–196.
[53] J.-Y. Sun, X. Zhao, W.R. Illeperuma, O. Chaudhuri, K.H. Oh, D.J. Mooney, J.J. Vlassak, Z. Suo, Highly stretchable and tough hydrogels, Nature 489 (7414) (2012) 133.
[54] P. Taddei, V. Chiono, A. Anghileri, G. Vozzi, G. Freddi, G. Ciardelli, Silk fibroin/gelatin blend films crosslinked with enzymes for biomedical applications, Macromol. Biosci. 13 (11) (2013) 1492–1510.
[55] S. Mohammadzadehmoghadam, Y. Dong, Fabrication and characterization of electrospun silk fibroin/gelatin scaffolds crosslinked with glutaraldehyde vapor, Front. Mater. 6 (2019) 1–12.
[56] S. Yan, Q. Wang, Z. Tariq, R. You, X. Li, M. Li, Q. Zhang, Facile preparation of bioactive silk fibroin/hyaluronic acid hydrogels, Int. J. Biol. Macromol. 118 (2018) 775–782.
[57] K. Luo, Y. Yang, Z. Shao, Physically crosslinked biocompatible silk-fibroin-based hydrogels with high mechanical performance, Adv. Funct. Mater. 26 (6) (2016) 872–880.
[58] H.J. Chun, C.H. Park, I.K. Kwon, G. Khang, Cutting-Edge Enabling Technologies for Regenerative Medicine, Springer, 2018.
[59] Y. Wang, B.J. Kim, B. Peng, W. Li, Y. Wang, M. Li, F.G. Omenetto, Controlling silk fibroin conformation for dynamic, responsive, multifunctional, micropatterned surfaces, Proc. Natl. Acad. Sci. 116 (43) (2019) 21361–21368.
[60] L. Hu, Y. Han, S. Ling, Y. Huang, J. Yao, Z. Shao, X. Chen, Direct observation of native silk fibroin conformation in silk gland of Bombyx mori Silkworm, ACS Biomater. Sci. Eng. (2020).
[61] Z. Zhu, S. Ling, J. Yeo, S. Zhao, L. Tozzi, M.J. Buehler, F. Omenetto, C. Li, D.L. Kaplan, High-Strength, Durable All-Silk Fibroin Hydrogels with Versatile Processability toward Multifunctional Applications, Adv. Funct. Mater. 28 (10) (2018) 1704757.
[62] K. Numata, D.L. Kaplan, Silk-based delivery systems of bioactive molecules, Adv. Drug Deliv. Rev. 62 (15) (2010) 1497–1508.
[63] D.T. Pham, W. Tiyaboonchai, Fibroin nanoparticles: a promising drug delivery system, Drug Deliv. 27 (1) (2020) 431–448.
[64] D.T. Pham, N. Saelim, W. Tiyaboonchai, Crosslinked fibroin nanoparticles using EDC or PEI for drug delivery: physicochemical properties, crystallinity and structure, J. Mater. Sci. 53 (20) (2018) 14087–14103.
[65] S. Chankow, S. Luemunkong, S. Kanokpanont, Conformational transitions of thai silk fibroin secondary structures, in: 2016 9th Biomedical Engineering International Conference (BMEiCON), IEEE, 2016, pp. 1–5.
[66] P. Dubey, S. Murab, S. Karmakar, P.K. Chowdhury, S. Ghosh, Modulation of self-assembly process of fibroin: an insight for regulating the conformation of silk biomaterials, Biomacromolecules 16 (12) (2015) 3936–3944.
[67] K. Kaewprasit, T. Kobayashi, S. Damrongsakkul, Alcohol-triggered silk fibroin hydrogels having random coil and β-turn structures enhanced for cytocompatible cell response, J. Appl. Polym. Sci. 137 (21) (2020) 48731.
[68] S. Keten, M.J. Buehler, Nanostructure and molecular mechanics of spider dragline silk protein assemblies, J. R. Soc. Interface 7 (53) (2010) 1709–1721.
[69] I. Bessonov, A. Moysenovich, A. Arkhipova, M. Ezernitskaya, Y. Efremov, V. Solodilov, P. Timashev, K. Shaytan, A. Shtil, M. Moisenovich, The mechanical properties, secondary structure, and osteogenic activity of photopolymerized fibroin, Polymers 12 (3) (2020) 646.
[70] A. Nova, S. Keten, N.M. Pugno, A. Redaelli, M.J. Buehler, Molecular and nanostructural mechanisms of deformation, strength and toughness of spider silk fibrils, Nano Lett. 10 (7) (2010) 2626–2634.
[71] S.S. Silva, A. Motta, M.T. Rodrigues, A.F. Pinheiro, M.E. Gomes, J.F. Mano, R.L. Reis, C. Migliaresi, Novel genipin-cross-linked chitosan/silk fibroin sponges for cartilage engineering strategies, Biomacromolecules 9 (10) (2008) 2764–2774.
[72] M. Fini, A. Motta, P. Torricelli, G. Giavaresi, N.N. Aldini, M. Tschon, R. Giardino, C. Migliaresi, The healing of confined critical size cancellous defects in the presence of silk fibroin hydrogel, Biomaterials 26 (17) (2005) 3527–3536.

[73] B.P. Partlow, C.W. Hanna, J. Rnjak-Kovacina, J.E. Moreau, M.B. Applegate, K.A. Burke, B. Marelli, A.N. Mitropoulos, F.G. Omenetto, D.L. Kaplan, Highly tunable elastomeric silk biomaterials, Adv. Funct. Mater. 24 (29) (2014) 4615–4624.

[74] B. Zhou, P. Wang, L. Cui, Y. Yu, C. Deng, Q. Wang, X. Fan, Self-crosslinking of silk fibroin using H 2 O 2-horseradish peroxidase system and the characteristics of the resulting fibroin membranes, Appl. Biochem. Biotechnol. 182 (4) (2017) 1548–1563.

[75] T.V. Chirila, S. Suzuki, C. Papolla, A comparative investigation of Bombyx mori silk fibroin hydrogels generated by chemical and enzymatic cross-linking, Biotechnol. Appl. Biochem. 64 (6) (2017) 771–781.

[76] J.N. Rodríguez-López, D.J. Lowe, J. Hernández-Ruiz, A.N. Hiner, F. García-Cánovas, R.N. Thorneley, Mechanism of reaction of hydrogen peroxide with horseradish peroxidase: identification of intermediates in the catalytic cycle, J. Am. Chem. Soc. 123 (48) (2001) 11838–11847.

[77] N.C. Veitch, Horseradish peroxidase: a modern view of a classic enzyme, Phytochemistry 65 (3) (2004) 249–259.

[78] D.J. Raven, C. Earland, M. Little, Occurrence of dityrosine in Tussah silk fibroin and keratin, Biochim. Biophys. Acta -Protein Struct. 251 (1) (1971) 96–99.

[79] L.P. Yan, J.M. Oliveira, A.L. Oliveira, R.L. Reis, Core-shell silk hydrogels with spatially tuned conformations as drug-delivery system, J. Tissue Eng. Regenerative Med. 11 (11) (2017) 3168–3177.

[80] H.J. Jin, J. Park, V. Karageorgiou, U.J. Kim, R. Valluzzi, P. Cebe, D.L. Kaplan, Water-stable silk films with reduced β-sheet content, Adv. Funct. Mater. 15 (8) (2005) 1241–1247.

[81] R. Nazarov, H.-J. Jin, D.L. Kaplan, Porous 3-D scaffolds from regenerated silk fibroin, Biomacromolecules 5 (3) (2004) 718–726.

[82] V.P. Ribeiro, J. Silva-Correia, C. Gonçalves, S. Pina, H. Radhouani, T. Montonen, J. Hyttinen, A. Roy, A.L. Oliveira, R.L. Reis, Rapidly responsive silk fibroin hydrogels as an artificial matrix for the programmed tumor cells death, PLoS ONE 13 (4) (2018).

[83] L.-P. Yan, J. Silva-Correia, V.P. Ribeiro, V. Miranda-Gonçalves, C. Correia, A. da Silva Morais, R.A. Sousa, R.M. Reis, A.L. Oliveira, J.M. Oliveira, Tumor growth suppression induced by biomimetic silk fibroin hydrogels, Sci. Rep. 6 (2016) 31037.

[84] X. Wang, Z. Ding, C. Wang, X. Chen, H. Xu, Q. Lu, D.L. Kaplan, Bioactive silk hydrogels with tunable mechanical properties, J. Mater. Chem. B 6 (18) (2018) 2739–2746.

[85] J. Yoo, E.D. Yeo, Y.K. Lee, Treatment of osteochondral lesions of the talus in Athletes, Korean J. Sports Med. 35 (2) (2017) 77–85.

[86] T.V. Chirila, S. Suzuki, O. Delcroix, Enzymatic crosslinking of Bombyx mori silk fibroin biomaterials: An investigation of the gel point by dynamic rheology, Biomater. Tissue Technol. 1 (1) (2017).

[87] H. De Azeredo, M. Rosa, M. De Sá, M. Souza Filho, K. Waldron, The use of biomass for packaging films and coatings, Advances in biorefineries, Elsevier; 2014, pp. 819-874.

[88] S.S. Silva, D. Maniglio, A. Motta, J.F. Mano, R.L. Reis, C. Migliaresi, Genipin-modified silk-fibroin nanometric nets, Macromol. Biosci. 8 (8) (2008) 766–774.

[89] Y.X. Wang, Y.P. Qin, Z.J. Kong, Y.J. Wang, L. Ma, Glutaraldehyde cross-linked silk fibroin films for controlled release, Advanced Materials Research, Trans Tech Publ, 2014, pp. 541–546.

[90] H. Heslot, Artificial fibrous proteins: a review, Biochimie 80 (1) (1998) 19–31.

[91] C. Tanaka, R. Takahashi, A. Asano, T. Kurotsu, H. Akai, K. Sato, D.P. Knight, T. Asakura, Structural analyses of Anaphe silk fibroin and several model peptides using 13C NMR and X-ray diffraction methods, Macromolecules 41 (3) (2008) 796–803.

[92] R. Yao, J. He, G. Meng, B. Jiang, F. Wu, Electrospun PCL/Gelatin composite fibrous scaffolds: mechanical properties and cellular responses, J. Biomater. Sci. Polym. Ed. 27 (9) (2016) 824–838.

[93] Y. Zhang, J. Venugopal, Z.-M. Huang, C.T. Lim, S. Ramakrishna, Crosslinking of the electrospun gelatin nanofibers, Polymer 47 (8) (2006) 2911–2917.

[94] J. Zhu, F. Yang, F. He, X. Tian, S. Tang, X. Chen, A tubular gelatin scaffold capable of the time-dependent controlled release of epidermal growth factor and mitomycin C, Colloids Surfaces B: Biointerfaces 135 (2015) 416–424.

[95] Y. Du, X.-Q. Gao, Z.-Y. Wang, D. Jin, S. Tong, X.-K. Wang, Construction and characterization of three-dimensional silk fibroin-gelatin scaffolds, J. Hard Tissue Biol. 25 (3) (2016) 269–276.

[96] S. Selvaraj, N.N. Fathima, Fenugreek Incorporated Silk Fibroin Nanofibers: A Potential Antioxidant Scaffold for Enhanced Wound Healing, ACS Appl. Mater. Interfaces 9 (7) (2017) 5916–5926.

[97] M. Simonet, N. Stingelin, J.G. Wismans, C.W. Oomens, A. Driessen-Mol, F.P. Baaijens, Tailoring the void space and mechanical properties in electrospun scaffolds towards physiological ranges, J. Mater. Chem. B 2 (3) (2014) 305–313.

[98] Y. Yin, D. Pu, J. Xiong, Analysis of the comprehensive tensile relationship in electrospun silk fibroin/polycaprolactone nanofiber membranes, Membranes 7 (4) (2017) 67.

[99] D.T. Cheung, M.E. Nimni, Mechanism of crosslinking of proteins by glutaraldehyde II. Reaction with monomeric and polymeric collagen, Connective Tissue Res. 10 (2) (1982) 201–216.

[100] A. Bigi, G. Cojazzi, S. Panzavolta, K. Rubini, N. Roveri, Mechanical and thermal properties of gelatin films at different degrees of glutaraldehyde crosslinking, Biomaterials 22 (8) (2001) 763–768.

[101] B. Ma, X. Wang, C. Wu, J. Chang, Crosslinking strategies for preparation of extracellular matrix-derived cardiovascular scaffolds, Regener. Biomater. 1 (1) (2014) 81–89.

[102] L. Fernández-García, N. Marí-Buyé, J.A. Barios, R. Madurga, M. Elices, J. Pérez-Rigueiro, M. Ramos, G.V. Guinea, D. González-Nieto, Safety and tolerability of silk fibroin hydrogels implanted into the mouse brain, Acta Biomater. 45 (2016) 262–275.

[103] H. Wu, S. Liu, L. Xiao, X. Dong, Q. Lu, D.L. Kaplan, Injectable and pH-responsive silk nanofiber hydrogels for sustained anticancer drug delivery, ACS Appl. Mater. Interfaces 8 (27) (2016) 17118–17126.

[104] B. Tavsanli, O. Okay, Mechanically robust and stretchable silk/hyaluronic acid hydrogels, Carbohydr. Polym. 208 (2019) 413–420.

[105] S. Nagarkar, T. Nicolai, C. Chassenieux, A. Lele, Structure and gelation mechanism of silk hydrogels, Phys. Chem. Chem. Phys. 12 (15) (2010) 3834–3844.

[106] D. Im, M. Kim, Y. Yoon, W. Park, Gelation behaviors and mechanism of silk fibroin according to the addition of nitrate salts, Int. J. Mol. Sci. 17 (10) (2016) 1697.

[107] N. Chantong, S. Damrongsakkul, J. Ratanavaraporn, Gelation process and physicochemical properties of thai silk fibroin hydrogels induced by various anionic surfactants for controlled release of curcumin, J. Surfactants Detergents (2019).

[108] Z. Yin, F. Wu, T. Xing, V.K. Yadavalli, S.C. Kundu, S. Lu, A silk fibroin hydrogel with reversible sol–gel transition, RSC Adv. 7 (39) (2017) 24085–24096.

[109] K. Deshmukh, M.B. Ahamed, R. Deshmukh, S.K. Pasha, P. Bhagat, K. Chidambaram, Biopolymer composites with high dielectric performance: interface engineering, Biopolymer Composites in Electronics, Elsevier; 2017, pp. 27–128.

[110] G. Kaur, J. Grewal, K. Jyoti, U.K. Jain, R. Chandra, J. Madan, Oral controlled and sustained drug delivery systems: Concepts, advances, preclinical, and clinical status, Drug Targeting and Stimuli Sensitive Drug Delivery Systems, Elsevier; 2018, pp. 567–626.

[111] C.H. Park, L. Jeong, D. Cho, O.H. Kwon, W.H. Park, Effect of methylcellulose on the formation and drug release behavior of silk fibroin hydrogel, Carbohydr. Polym. 98 (1) (2013) 1179–1185.

[112] P. Nasatto, F. Pignon, J. Silveira, M. Duarte, M. Noseda, M. Rinaudo, Methylcellulose, a cellulose derivative with original physical properties and extended applications, Polymers 7 (5) (2015) 777–803.

[113] S. Das, F. Pati, Y.-J. Choi, G. Rijal, J.-H. Shim, S.W. Kim, A.R. Ray, D.-W. Cho, S. Ghosh, Bioprintable, cell-laden silk fibroin–gelatin hydrogel supporting multilineage differentiation of stem cells for fabrication of three-dimensional tissue constructs, Acta Biomater. 11 (2015) 233–246.

[114] A. Radosavljević, J. Spasojević, J. Krstić, Z. Kačarević-Popović, Nanocomposite Hydrogels Obtained by Gamma Irradiation, Cellulose-Based Superabsorbent Hydrogels (2019) 601–623.

[115] M. Tavakol, E. Vasheghani-Farahani, M.A. Mohammadifar, M. Dehghan-Niri, Effect of gamma irradiation on the physicochemical and rheological properties of enzyme-catalyzed tragacanth-based injectable hydrogels, J. Polym. Eng. 39 (5) (2019) 442–449.

[116] L. Davison, E. Themistou, F. Buchanan, E. Cunningham, Low temperature gamma sterilization of a bioresorbable polymer, PLGA, Radiation Phys. Chem. 143 (2018) 27–32.

[117] J.M. Patel, R.C. Jackson, G.L. Schneider, S.A. Ghodbane, M.G. Dunn, Carbodiimide cross-linking counteracts the detrimental effects of gamma irradiation on the physical properties of collagen-hyaluronan sponges, J. Mater. Sci. - Mater. Med. 29 (6) (2018) 75.

[118] M.H. Kim, W.H. Park, Chemically cross-linked silk fibroin hydrogel with enhanced elastic properties, biodegradability, and biocompatibility, Int. J. Nanomed. 11 (2016) 2967.

[119] S.Y. Xiong, Y.M. Xu, Y.H. Jiao, L. Wang, M.Z. Li, Effects of gamma irradiation on the structure and mechanical properties of wild silkworms and bombyx mori silk fibroin films, Advanced Materials Research, Trans Tech Publ, 2011, pp. 27–31.

[120] M. Tsukada, G. Freddi, N. Minoura, Changes in the fine structure of silk fibroin fibers following gamma irradiation, J. Appl. Polym. Sci. 51 (5) (1994) 823–829.

[121] H. Jin, H. Yin, A. Yan, The effect of gamma ray on the thermo-mechanical property of silk fibroin, Therm. Sci. 17 (5) (2013) 1521–1522.

[122] H. Jin, Study on biocompatibility and biodegradation of silk fibroin degraded by γ-Rays in vivo, J. Radiation Res. Radiation Process. 31 (1) (2013).

[123] M.A. Koperska, D. Pawcenis, J.M. Milczarek, A. Blachecki, T. Łojewski, J. Łojewska, Fibroin degradation–Critical evaluation of conventional analytical methods, Polym. Degradation Stability 120 (2015) 357–367.

[124] A. Sionkowska, A. Planecka, The influence of UV radiation on silk fibroin, Polym. Degradation Stability 96 (4) (2011) 523–528.

[125] S. Baltova, V. Vassileva, E. Valtcheva, Photochemical behaviour of natural silk—I. Kinetic investigation of photoyellowing, Polym. Degradation Stability 60 (1) (1998) 53–60.

[126] S. Baltova, V. Vassileva, Photochemical behaviour of natural silk—II. Mechanism of fibroin photodestruction, Polym. Degradation stability 60 (1) (1998) 61–65.

[127] R. Kuruppillai, S. Hersch, P. Tucker, Degradation of silk by heat and light, Abstracts of papers, 1985.

[128] H. Liu, S. Zhao, Q. Zhang, T. Yeerken, W. Yu, Secondary structure transformation and mechanical properties of silk fibers by ultraviolet irradiation and water, Text. Res. J. 89 (14) (2019) 2802–2812.

[129] A. Maziz, O. Leprette, L. Boyer, C. Blatché, C. Bergaud, Tuning the properties of silk fibroin biomaterial via chemical cross-linking, Biomed. Phys. Eng. Express 4 (6) (2018) 065012.

[130] J.C. Bragg, H. Kweon, Y. Jo, K.G. Lee, C.C. Lin, Modulating properties of chemically crosslinked PEG hydrogels via physical entrapment of silk fibroin, J. Appl. Polym. Sci. 133 (9) (2016).

[131] D. Su, M. Yao, J. Liu, Y. Zhong, X. Chen, Z. Shao, Enhancing mechanical properties of silk fibroin hydrogel through restricting the growth of β-sheet domains, ACS Appl. Mater. Interfaces 9 (20) (2017) 17489–17498.

[132] A. Sionkowska, A. Płanecka, K. Lewandowska, M. Michalska, The influence of UV-irradiation on thermal and mechanical properties of chitosan and silk fibroin

mixtures, J. Photochem. Photobiol. B: Biol. 140 (2014) 301–305.
[133] I.V. Bessonov, Y.A. Rochev, A.Y. Arkhipova, M.N. Kopitsyna, D.V. Bagrov, E.A. Karpushkin, T.N. Bibikova, A.M. Moysenovich, A.S. Soldatenko, I.I. Nikishin, Fabrication of hydrogel scaffolds via photocrosslinking of methacrylated silk fibroin, Biomed. Mater. 14 (3) (2019) 034102.
[134] Z. Wen, F. Jiang, F. Wu, Z. Yin, K. Kaur, J. Chakraborty, S. Ghosh, S. Lu, Photocurable silk fibroin-polyvinylpyrrolidone hydrogel, Materialia (2019) 100525.
[135] H. Wei, A.Y. Zhang, L. Qian, H. Yu, D. Hou, R. Qiu, Z.G. Feng, Supramolecular structured hydrogel preparation based on self-assemblies of photocurable star-shaped macromers with α-cyclodextrins, J. Polym. Sci., Part A: Polym. Chem. 43 (13) (2005) 2941–2949.
[136] M.B. Applegate, B.P. Partlow, J. Coburn, B. Marelli, C. Pirie, R. Pineda, D.L. Kaplan, F.G. Omenetto, Photocrosslinking of silk fibroin using riboflavin for ocular prostheses, Adv. Mater. 28 (12) (2016) 2417–2420.
[137] S. Ibusuki, G.J. Halbesma, M.A. Randolph, R.W. Redmond, I.E. Kochevar, T.J. Gill, Photochemically cross-linked collagen gels as three-dimensional scaffolds for tissue engineering, Tissue Eng. 13 (8) (2007) 1995–2001.
[138] S.H. Kim, C.C. Chu, Fabrication of a biodegradable polysaccharide hydrogel with riboflavin, vitamin B2, as a photo-initiator and L-arginine as coinitiator upon UV irradiation, J. Biomed. Mater. Res. B Appl. Biomater. 91 (1) (2009) 390–400.
[139] A.K. Nguyen, S.D. Gittard, A. Koroleva, S. Schlie, A. Gaidukeviciute, B.N. Chichkov, R.J. Narayan, Two-photon polymerization of polyethylene glycol diacrylate scaffolds with riboflavin and triethanolamine used as a water-soluble photoinitiator, Regenerative Med. 8 (6) (2013) 725–738.
[140] C. Jarry, C. Chaput, A. Chenite, M.A. Renaud, M. Buschmann, J.C. Leroux, Effects of steam sterilization on thermogelling chitosan-based gels, J. Biomed. Mater. Res.: Off. J. Soc. Biomater., Japanese Soc. Biomater., Aust. Soc. Biomater. Korean Soc. Biomater. 58 (1) (2001) 127–135.
[141] L. Costa, M. Luda, L. Trossarelli, E.B. Del Prever, M. Crova, P. Gallinaro, Oxidation in orthopaedic UHMWPE sterilized by gamma-radiation and ethylene oxide, Biomaterials 19 (7–9) (1998) 659–668.
[142] G.C. Mendes, T.R. Brandao, C.L. Silva, Ethylene oxide sterilization of medical devices: a review, Am. J. Infect. Control 35 (9) (2007) 574–581.
[143] Y.M. Yang, Y.H. Zhao, X.H. Liu, F. Ding, X.S. Gu, The effect of different sterilization procedures on chitosan dried powder, J. Appl. Polym. Sci. 104 (3) (2007) 1968–1972.
[144] Y. Zhao, X. Yan, F. Ding, Y. Yang, X. Gu, The effects of different sterilization methods on silk fibroin, J. Biomed. Sci. Eng. 4 (05) (2011) 397.
[145] G. Najafpour, Biochemical engineering and biotechnology, Elsevier, 2015.
[146] J. Gatesy, C. Hayashi, D. Motriuk, J. Woods, R. Lewis, Extreme diversity, conservation, and convergence of spider silk fibroin sequences, Science 291 (5513) (2001) 2603–2605.
[147] C. Fu, D. Porter, Z. Shao, Moisture effects on Antheraea pernyi silk's mechanical property, Macromolecules 42 (20) (2009) 7877–7880.
[148] Y. Cheng, L.-D. Koh, D. Li, B. Ji, M.-Y. Han, Y.-W. Zhang, On the strength of β-sheet crystallites of Bombyx mori silk fibroin, J. R. Soc. Interface 11 (96) (2014) 20140305.
[149] C.Z. Zhou, F. Confalonieri, M. Jacquet, R. Perasso, Z.G. Li, J. Janin, Silk fibroin: structural implications of a remarkable amino acid sequence, Proteins: Struct. Function, Bioinform. 44 (2) (2001) 119–122.
[150] K.Y. Lee, D.J. Mooney, Hydrogels for tissue engineering, Chem. Rev. 101 (7) (2001) 1869–1880.
[151] I. Krasnov, I. Diddens, N. Hauptmann, G. Helms, M. Ogurreck, T. Seydel, S.S. Funari, M. Müller, Mechanical properties of silk: interplay of deformation on macroscopic and molecular length scales, Phys. Rev. Lett. 100 (4) (2008) 048104.
[152] M. Cetinkaya, S. Xiao, B. Markert, W. Stacklies, F. Gräter, Silk fiber mechanics from multiscale force distribution analysis, Biophys. J . 100 (5) (2011) 1298–1305.
[153] X. Huang, S. Fan, A.I.M. Altayp, Y. Zhang, H. Shao, X. Hu, M. Xie, Y. Xu, Tunable structures and properties of electrospun regenerated silk fibroin mats annealed in water vapor at different times and temperatures, J. Nanomater. 2014 (2014) 7.
[154] M. Gholipourmalekabadi, A. Samadikuchaksaraei, A.M. Seifalian, A.M. Urbanska, H. Ghanbarian, J.G. Hardy, M.D. Omrani, M. Mozafari, R.L. Reis, S.C. Kundu, Silk fibroin/amniotic membrane 3D bi-layered artificial skin, Biomed. Mater. 13 (3) (2018) 035003.
[155] L. Fan, H. Wang, K. Zhang, C. He, Z. Cai, X. Mo, Regenerated silk fibroin nanofibrous matrices treated with 75% ethanol vapor for tissue-engineering applications, J. Biomater. Sci. Polym. Ed. 23 (1–4) (2012) 497–508.
[156] B.M. Min, L. Jeong, K.Y. Lee, W.H. Park, Regenerated silk fibroin nanofibers: Water vapor-induced structural changes and their effects on the behavior of normal human cells, Macromol. Biosci. 6 (4) (2006) 285–292.
[157] X. Hu, K. Shmelev, L. Sun, E.-S. Gil, S.-H. Park, P. Cebe, D.L. Kaplan, Regulation of silk material structure by temperature-controlled water vapor annealing, Biomacromolecules 12 (5) (2011) 1686–1696.
[158] S. Fan, Y. Zhang, H. Shao, X. Hu, Electrospun regenerated silk fibroin mats with enhanced mechanical properties, nternational, J. Biol. Macromol. 56 (2013) 83–88.
[159] B.D. Lawrence, S. Wharram, J.A. Kluge, G.G. Leisk, F.G. Omenetto, M.I. Rosenblatt, D.L. Kaplan, Effect of hydration on silk film material properties, Macromol. Biosci. 10 (4) (2010) 393–403.
[160] K. Yazawa, K. Ishida, H. Masunaga, T. Hikima, K. Numata, Influence of water content on the β-sheet formation, thermal stability, water removal, and mechanical properties of silk materials, Biomacromolecules 17 (3) (2016) 1057–1066.
[161] S. Putthanarat, S. Zarkoob, J. Magoshi, J. Chen, R. Eby, M. Stone, W. Adams, Effect of processing temperature on the morphology of silk membranes, Polymer 43 (12) (2002) 3405–3413.
[162] Z. Hadisi, J. Nourmohammadi, N. Haghighipour, S. Heidari, How direct electrospinning in methanol bath affects the physico-chemical and biological properties of silk fibroin nanofibrous scaffolds, Micro Nano Lett. 11 (9) (2016) 514–517.
[163] D. Terada, Y. Yokoyama, S. Hattori, H. Kobayashi, Y. Tamada, The outermost surface properties of silk fibroin films reflect ethanol-treatment conditions used in biomaterial preparation, Mater. Sci. Eng.: C 58 (2016) 119–126.
[164] E. Sashina, A. Bochek, N. Novoselov, D. Kirichenko, Structure and solubility of natural silk fibroin, Russ. J. Appl. Chem. 79 (6) (2006) 869–876.
[165] M. Garcia-Fuentes, E. Giger, L. Meinel, H.P. Merkle, The effect of hyaluronic acid on silk fibroin conformation, Biomaterials 29 (6) (2008) 633–642.
[166] N. Amiraliyan, M. Nouri, M.H. Kish, Structural characterization and mechanical properties of electrospun silk fibroin nanofiber mats, Polym. Sci. Series A 52 (4) (2010) 407–412.
[167] S. Yan, G. Han, Q. Wang, S. Zhang, R. You, Z. Luo, A. Xu, X. Li, M. Li, Q. Zhang, Directed assembly of robust and biocompatible silk fibroin/hyaluronic acid composite hydrogels, Compos. B Eng. 176 (2019) 107204.
[168] K. Kaewprasit, T. Kobayashi, S. Damrongsakkul, Thai silk fibroin gelation process enhancing by monohydric and polyhydric alcohols, Int. J. Biol. Macromol. 118 (2018) 1726–1735.
[169] S. Midha, S. Kumar, A. Sharma, K. Kaur, X. Shi, P. Naruphontjirakul, J.R. Jones, S. Ghosh, Silk fibroin-bioactive glass based advanced biomaterials: towards patient-specific bone grafts, Biomed. Mater. 13 (5) (2018) 055012.
[170] C. Jiang, X. Wang, R. Gunawidjaja, Y.H. Lin, M.K. Gupta, D.L. Kaplan, R.R. Naik, V.V. Tsukruk, Mechanical properties of robust ultrathin silk fibroin films, Adv. Funct. Mater. 17 (13) (2007) 2229–2237.
[171] A. Motta, L. Fambri, C. Migliaresi, Regenerated silk fibroin films: thermal and dynamic mechanical analysis, Macromol. Chem. Phys. 203 (10–11) (2002) 1658–1665.